Friction https://mc03.manuscriptcentral.com/friction

https://doi.org/10.26599/FRICT.2026.9441248

Review Article

Designs and applications of nitride coatings to hot metal forming dies

Kuniaki Dohda [1*], Tatsuhiko Aizawa [2], Tatsuya Funazuka [3*], Panuwat Soranansri [4*], And Keishi Okamoto [5]

[1] *Department of Mechanical Engineering, Northwestern University, Evanston 60201, USA*

[2] *Surface Engineering Design Laboratory, Shibaura Institute of Technology, Tokyo 144-0045, Japan*

[3] *Faculty of Engineering, University of Toyama, Toyama 930-8555, Japan*

[4] *Department of Teacher Training in Mechanical Engineering, Faculty of Technical Education, King Mongkut's University of Technology North Bangkok, Bangkok 10800, Thailand*

[5] *Toyo Advanced Technologies Co. Ltd., Hiroshima 734-8501, Japan*

[*]Corresponding author: Kuniaki DOHDA, E-mail: dohda.kuni@northwestern.edu

Tatsuya FUNAZUKA, E-mail: funazuka@eng.u-toyama.ac.jp

Panuwat SORANANSRI, E-mail: panuwat.s@fte.kmutnb.ac.th

Received: September 9, 2025; Revised: February 20, 2026; Accepted: April 1, 2026

Abstract

Thin film coatings are widely applied to extend the service life of hot metal forming dies by improving wear resistance, reducing friction, and mitigating thermal and chemical damage. Nitride

coatings deposited by Physical Vapor Deposition (PVD) and Chemical Vapor Deposition (CVD) methods have demonstrated potential to deal with critical challenges at the die-workpiece interface. This paper reviews the designs and applications of nitride coatings to hot metal forming dies. The discussion begins with the fundamentals and characteristics of monolithic, binary, and laminated coatings, which aim to enhance tribological performance at the interface. It then explores the application of nitride coatings used in the hot forming processes of steels, aluminum alloys, and other metal alloys. Finally, the review concludes with key highlights and recommendations for coatings selection and future research to improve the tribological performance of hot metal forming dies.

Keywords: Friction, Galling, PVD and CVD coatings, Hot forming process, Steels, Aluminum alloys

1 Introduction

A coating is a thin layer of material deposited on various substrates to enhance their surface properties and textures. The typical thickness ranges from submicron to several hundred microns, depending on its deposition method and application [1]. By improving the surface properties and textures, the coating can increase wear resistance, reduce friction, and protect against thermal and chemical damage. Due to these positive aspects, thin film coatings are widely used in numerous applications. For instance, in the mining industry, the rock drilling tool is coated with tungsten carbide (WC) or diamond-like carbon (DLC) to improve the wear resistance. This results in expanding its service life and consequently reduces its maintenance cost [2,3]. Additionally, in the turbine engine, duplex layers of coating, consisting of a metallic bond layer and a ceramic top layer, are applied as the thermal insulator and barrier for the components that work in hot gas conditions. It leads to achieving their functional requirements [4].

This paper mainly focuses on the nitride coatings for hot metal forming dies. In general, the dies are subjected to severe contact loads. For example, the contact pressure is close to or above the yield stress of formed materials at operating temperatures. Moreover, their surface also needs to contact the hot billet. The temperature is around 1,100°C to 1,250°C for steel forming and 400°C to 500°C for aluminum forming [5]. It causes the interface temperature, such as the hot forging process of steel, to reach 700°C to 800°C [6]. The relative sliding velocity can also be up to 1,000 mm/s [7]. Due to the elevated temperatures, the oxidation of materials leads to the formation of hard and brittle oxide layers [8]. These layers fracture during the deformation of the workpiece and then cause abrasive wear on the die surface [7]. Furthermore, galling is another common issue in metal forming as a result of direct contact between the die and workpiece under high contact pressure. It generates defects in the workpiece surface [9]. Normally, the interface in the hot forming of aluminum alloys is less severe due to lower yield stress and operating temperature. Nonetheless, the strong chemical affinity between aluminum alloys and tool materials results in more severe galling. Thus, the coating functionalities of dies in the hot forming of steels and aluminum alloys are slightly different.

Physical Vapor Deposition (PVD) and Chemical Vapor Deposition (CVD) nitride coatings are suitable coating technologies for hot metal forming dies. The dies can be coated with various nitride coatings, such as TiN, CrN, and TiAlN. The general criteria for selecting those coatings include substrate materials, operating conditions, and cost-effectiveness. For instance, Widomski et al. [10] applied the hybrid layers of coating, composed of nitriding and Cr/CrN layers, to improve the service life of the die in the industrial hot forging process of an automotive component. Those hybrid layers can increase the service life of the die by 80% when compared to the conventional nitriding die. It is because the Cr/CrN layer can maintain high hardness for more forging cycles. On the other hand, Funazuka et al. [11] have been successful in suppressing the tearing defects in the hot extrusion process of AA7075 aluminum alloy by using the AlCrN coating die instead of the conventional nitriding die. The AlCrN coating can reduce the frictional stress at the die-workpiece

interface. Those two examples show that dissimilar PVD nitride coatings are used for specific hot forming processes. Therefore, understanding the differences between numerous nitride coatings can help in selecting the appropriate coating for hot metal forming dies.

This paper reviews the designs and applications of nitride coatings to hot metal forming dies. The content begins by exploring the nitride coating design, covering both fundamentals and characteristics of monolithic, binary, and laminated coatings to enhance tribological performance. Then, it examines the nitride coatings used in the hot forming process of steels, aluminum alloys, and other metal alloys. Finally, conclusions with highlights and recommendations for future research are provided.

2 Design of Nitride Coating for Hot Metal Forming Dies

Various nitride and oxide coatings have been developed to improve the wear toughness of metal forming dies and tools [12]. In particular, the monolithic nitride coating, such as TiN, TiCN, and CrN, was first employed as a protective surface layer of the cutting and drilling tools [13], the punches in stamping [14], and the piston rings [15]. However, these monolithic nitrides often had insufficient heat resistance and suffered from oxidation wear in hot metal forming [16,17]. Aluminum was selected as the second metallic element in the binary nitride coating design, such as TiAlN and CrAlN [18,19]. They had sufficient hardness and oxidation resistance at elevated temperatures for usage in hot extrusion [20], hot forging [21], and hot stamping [22]. In addition to the ternary and quaternary alloying design on the nitride coating [23], a nano-lamination of binary nitride layers as well as multi-layer coating of monolithic and binary nitride films, provided an innovative way to improve the wear resistance even at elevated temperatures [24–26]. A comprehensive understanding of the importance on the alloying design of nitrides and their nanostructuring became a key to finding a solution for the improvement of wear resistance in hot metal forming by the nitride coating [27,28].

2.1 Characteristics of Monolithic Nitride Coating in Crystallography and Tribology

TiN by PVD has been utilized as a typical protective coating of dies. As stated in [29], the physically vapor-deposited films are characterized by the microstructural model as a function of the working pressure and temperature during PVD. In the normal PVD process at the lower pressure and temperature, a deposited nitride film grows in a columnar structure according to the Thornton structure model. As shown in Fig. 1a, TiN coating has a dense columnar structure with a thickness of 1 μm on the dis substrate. Its Selected Area Electron Diffraction (SAED) image is depicted in Fig. 1b. Fine bright spots in each crystallographic plane of TiN (111), (220), (221), and (311) reveal that this stoichiometric TiN consists of dense and fine grains. The lattice parameter (Λ) of this nano-columnar TiN coating is 0.42520 nm, while Λ = 0.42580 nm in the bulk sintered TiN with the equiaxial structure in [30]. Due to the columnar growth of the TiN layer on the substrate, its preferable crystallographic orientation is controllable by the PVD processing conditions.

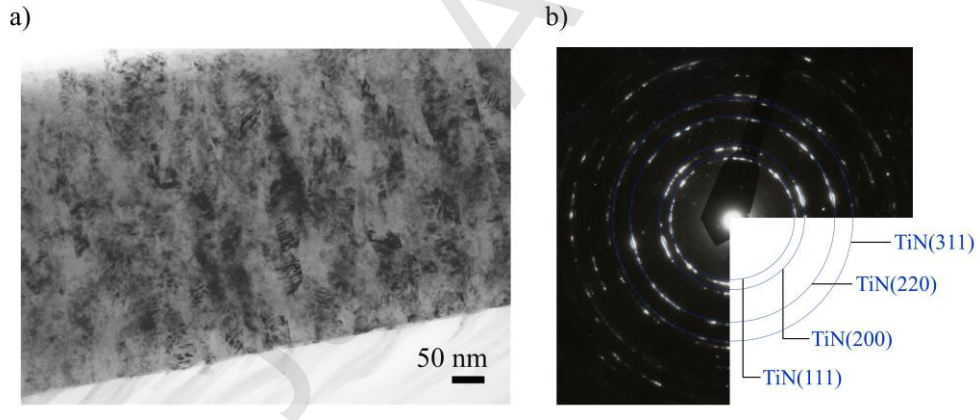

Fig. 1 The crystallographic structure of PVD TiN coating on the substrate: a) Cross-sectional TEM image of the nano-columnar TiN film, and b) bright-field image of the columnar-structured TiN by SAED.

To investigate the tribological performance of the columnar TiN coating, the Ball-on-Disc (BOD) test was employed to describe the variation of the friction coefficient (μ) with distance (L). As shown in Fig. 2a, μ = 0.8 ~ 1.2 in the whole distance against the counter material of the AISI304 ball with a diameter of 6 mm when the applied load was 2 N. In general, the physical surface treatment via the bombardment by the ion implantation was effective in reducing this high friction coefficient [31]. The argon ions were implanted into the as-deposited TiN coating with a dose of 1.0 x 10^{17} ions/cm^2. However, no improvement in friction was observed in Fig. 2a. When changing the counter material from AISI304 to pure titanium, this high frictional state was much enhanced to have μ > 2.0 [32]. Figure 2b depicts the wear track of TiN coating after running 50 m under the applied load of 2 N and the sliding velocity of 0.02 m/s. Severe abrasive wear took place in the contact track of the TiN coating surface to the counter materials. TiN film was eroded from the center of the track to its end with oxidation from TiN to TiO_2. The above high friction and wear of the as-deposited TiN coating comes from its local galling to the AISI304 ball in the BOD test. The local oxidation of TiN at hot spots in the contact track grows to fatal abrasive wear.

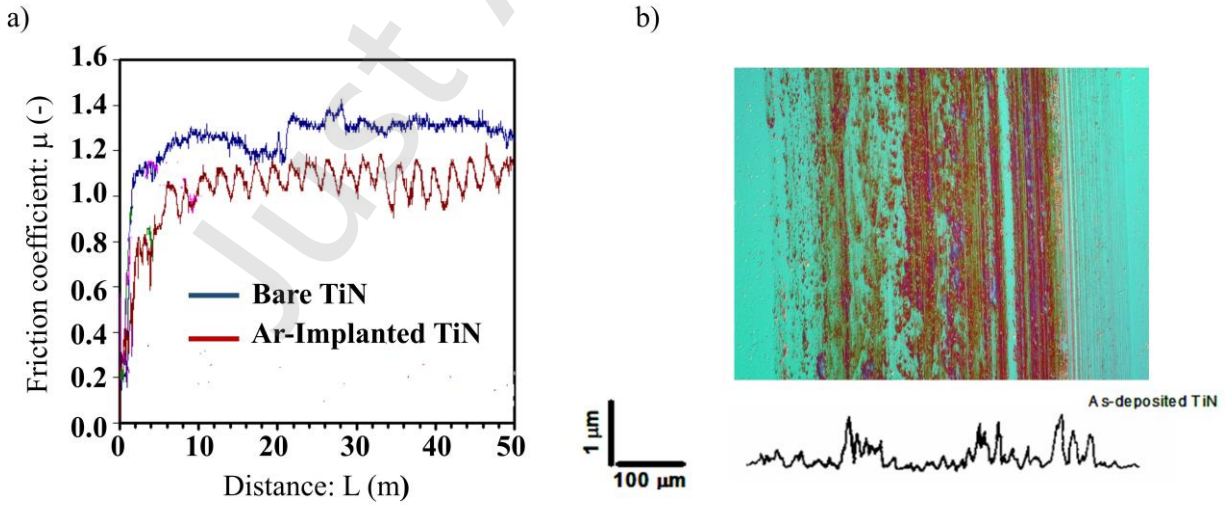

Fig. 2 Tribological performance of the as-deposited TiN coating by the BOD test: a) Variation of the friction coefficient with the distance, and b) wear track of TiN coating after running 50 m under the applied load of 2 N and the sliding velocity of 0.02 m/s.

In the monolithic nitride coating, its tribological behavior is strongly dependent on the binding state between the constituent cation and nitrogen atoms. Tanium in TiN was changed to chromium in CrN to investigate the effect of this cation exchange on the tribological performance. In addition, the film thickness (h) of this CrN was varied from submicron to 50 μm to investigate the effect of coating thickness on the tribological performance. The duplex coating scheme was employed to build up a surface layer on the AISI434 stainless steel disc with a size of 30 mm in diameter and 5 mm in thickness. As depicted in Fig. 3a, the polished AISI434 substrate with a hardness of 250 HV was first gas-nitrided to have an average hardness of 700 HV instead of heat treatment. The gas-nitrided layer thickness was 100 μm. Next, CrN was deposited onto the nitrided layer to have an average hardness of 1400 HV and a coating thickness of 10 μm. As shown in Fig. 3b, the CrN film has a columnar structure, similar to TiN coating in Fig. 1.

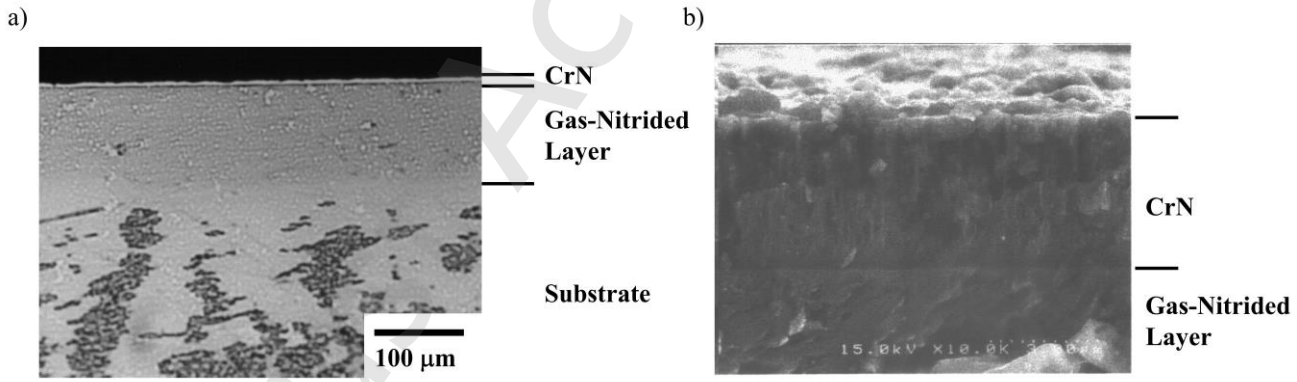

Fig. 3 Microstructure of CrN coated AISI434 stainless steel substrate: a) Cross-sectional view, and b) SEM image of cross-section.

The BOD test was also utilized with the use of the AISI304 ball. Its diameter was 6 mm. The average friction coefficient and the wear volume (W_V) were measured after the stationary running in 100 m. The applied load (P) and the sliding velocity (v) were varied from 2 N to 10 N and from 0.01 to 0.50 m/s, respectively. Figure 4a depicts the variation of the friction coefficient with the film

thickness under the constant applied load of 2 N, 5 N, and 10 N, respectively. When h = 0, the gas-nitrided AISI434 disc was used in the BOD test, while the CrN/Cr_2N sintered bulk disc [33] was used in testing when h = 50 μm. When P = 2 N, μ ~ 0.53 on average with less dependence on the film thickness. This friction coefficient slightly increases with P; e.g., when P = 10 N, μ ~ 0.7 to 0.8. The wear damage of the disc is accelerated during the running process to a distance of 50 m during the BOD test. Figure 4b shows the dependence of the specific wear volume (W_s) on the CrN film thickness. Here, W_s was defined by $W_s = W_v / (P \cdot v)$ for the measured wear volume (W_v). In general, the abrasive wear takes place when W_s ranges from 10^{-11} to 10^{-13} m^2/N, while it turns to be adhesive when 10^{-12} $m^2/N > W_s > 10^{-16}$ m^2/N. In Fig. 4b, W_s slightly increases with h in its range of 10^{-14} m^2/N. The adhesive wear increases with h in this BOD test between the AISI304 ball and CrN coating. The mass gain by oxidation, as well as the mass transfer from the counter material, occurs on the contact interface between them. To be noticed, this increase of Ws with h also reveals that the hardness of CrN coating is still insufficient as a protective duplex system and that a composite of Cr_2N to CrN in bulk has a trend to increase the wear volume.

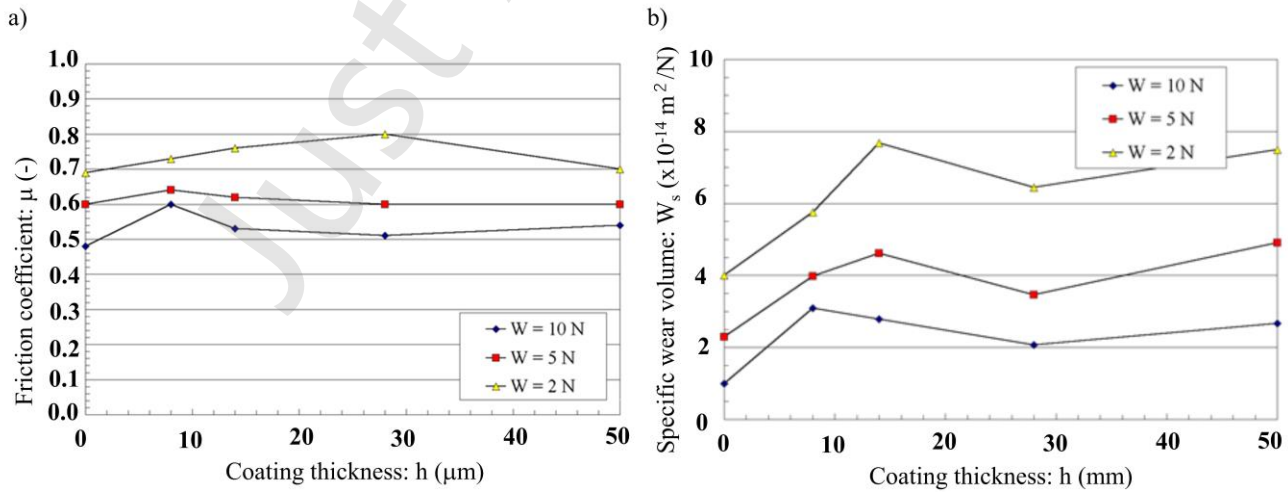

Fig. 4 Tribological performance of CrN coated AISI434 stainless steels: a) Variation of the friction coefficient with increasing the film thickness under the applied load of 2 N, 5 N, and 10 N, and b)

Variation of the specific wear volume with increasing the film thickness under the applied load of 2 N, 5 N, and 10 N.

The SEM was employed to observe the surface morphology of CrN coatings after running for 100 mm in the BOD test. Figures 5a - d show the variation of the CrN contact surface to the counter ball with increasing sliding velocity. Figures 5a - c depict the abrasively worn surfaces, while the medium oxidation took place for v > 0.1 m/s, as shown in Fig. 5d. Figure 5e also shows the mildly oxidized CrN/Cr_2N bulk when v = 0.2 m/s. This onset of oxidation is responsible for the increase of the specific wear volume in the order of 10^{-14} m^2/N in Fig. 4b. This difference of severity in the oxidation wear between the CrN coating and bulk CrN/Cr_2N comes from the thermal diffusivity in the columnar structure of the CrN coating. Since the effective thermal diffusion coefficient increases with the reduction of the grain size, the specific wear volume increases in the high sliding velocity range [34].

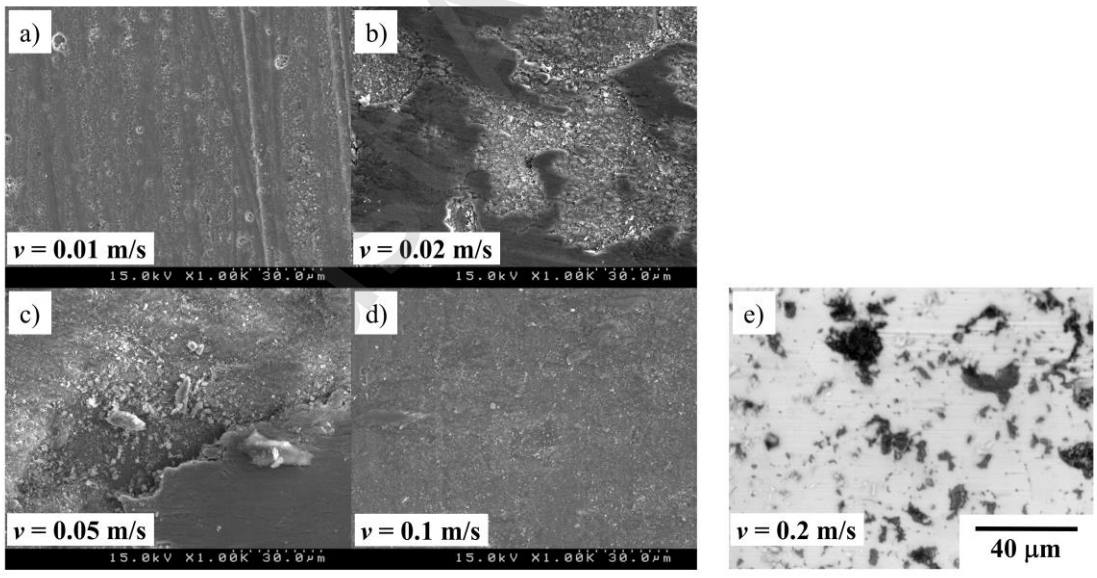

Fig. 5 Change of the wearing process for CrN coating with increasing the sliding velocity, being compared to the abrasive wearing of bulk CrN: a) - d) Morphology of worn surface for CrN coating, and e) abrasively worn surface of bulk CrN.

TiN and CrN coated dies and tools in the cold and dry metal forming experience high friction and oxidation wear. The tribological performance is enhanced during the hot metal forming by the accelerated oxidation process on the contact interface between the nitride coating and the work materials. Their oxidation mechanism must be considered in the design of nitride coatings to work in hot metal forming.

2.2 Oxidation Wear of Monolithic Nitride Coating

As stated in 2.1, the monolithic nitride coating is subjected to oxidation wear even in cold conditions. Its tribological behavior is affected by its oxidation in air under hot conditions. High temperature oxidation tests were carried out by the thermo-gravimetric analyzer (Shimadzu TGA-51H) in a dry oxygen atmosphere in the temperature range from 600˚C to 800˚C. The holding time was constant at 20 h. The heating rate was 20˚C/min, and the flow rate of oxygen was 20 cm^3/min. The mass gain of each specimen was recorded with time when heating the specimen to the holding temperature, soaking, and cooling down to room temperature.

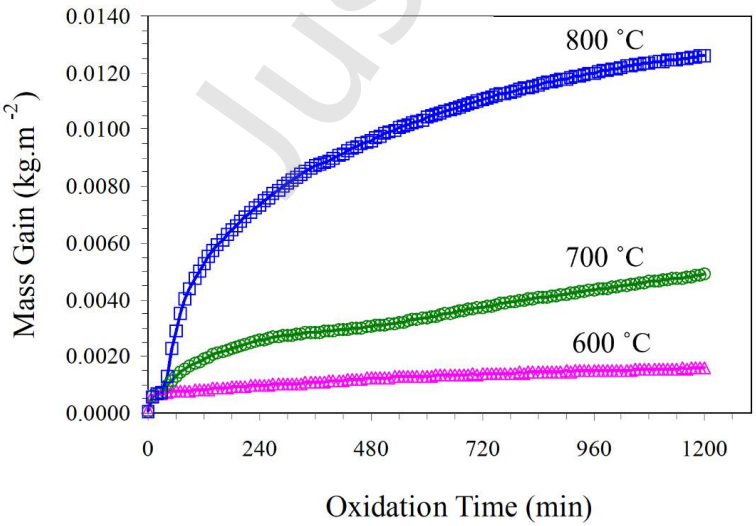

Fig. 6 Time evolution of the mass gain for the as-deposited TiN coatings at the holding temperatures of 600˚C, 700˚C, and 800˚C.

Figure 6 depicts the time evolution of mass gain for TiN coated AISI304 substrates under the oxygen atmosphere at the holding temperatures of 600˚C, 700˚C, and 800˚C, respectively. Even at 600˚C, the mass gain increases with time in a parabolic trend. The significant oxidation took place from the surface to the depth of the TiN film. These parabolic mass-gain curves are enhanced by increasing the holding temperature to 700˚C and 800˚C, respectively. X-ray Diffraction (XRD) was utilized to characterize this oxidized TiN after oxidation testing for 20 h at 600˚C. No TiN was detected, but the surface of bare TiN fully changed to TiO_2. This proves that the as-deposited TiN coating has lower heat resistance in air. In addition to this oxidation from TiN to TiO_2, Fe_2O_3 was also detected after testing at 700˚C and 800˚C. Severe oxidation took place to induce the penetrating cracking into the oxidized TiN film. Iron (Fe) diffused from the AISI304 substrate through these cracks and reacted with oxygen to synthesize iron oxides at the surface.

In this oxidation process, the mass gain (ΔM) of the TiN coating is governed by the power law as follows:

$$(\Delta M/S) = K \cdot t^{n} \quad (1)$$

where S is the area of oxidation, t is the time, n is the power exponent, and K is a parameter, which is further expressed by the Arrhenius relation,

$$K = K_o \cdot e^{-Ea/RT} \quad (2)$$

where K_o is the proper rate coefficient, R is the gas constant, T is the temperature (K), and E_a is the activation energy. This E_a plays a role in evaluating the heat resistant capacity of the coating against oxidation. If E_a is small, the oxidation takes place easily to fully oxidize the coating materials. On the other hand, the coating with higher E_a has enough toughness to suppress the oxidation process. E_a = 167 kJ/mol for the TiN coating in the oxygen atmosphere [17] and E_a = 136 kJ/mol in air [35]. These

low activation energies imply that the as-deposited TiN coating has low oxidation toughness, so that its usage for hot metal forming is strictly limited in practice.

There are two ways to improve the low oxidation toughness of TiN. As mentioned above, titanium is changed to chromium to suppress the oxidation of nitride coating at hot spots on its contact interface to counter material [33,34]. Next, the second metallic element is included in the alloying design to promote the heat resistance at hot metal forming.

2.3 Role of Aluminum in the Alloying Design of Nitride Coating

In this selection, what kind of cation element is employed in the alloying design of the nitride coating is considered. Aluminum is selected as an element with a relatively smaller atomic radius than titanium among several candidates [17,36]. The charge transfer from metallic atoms to nitrogen atoms is reduced via this substitution of titanium atoms by aluminum ones. Then, the effective size of the N-sublattice is also reduced in TiN. The aluminum implantation process was employed to investigate the role of aluminum in changing the crystallographic system, the hardness, and the oxidation toughness.

First, the lattice parameter as well as the residual stress were measured for each Al-implanted TiN film with different aluminum doses. In case of aluminum implantation to TiN coating with the nano-columnar structure, as shown in Fig. 1, its lattice parameter (Λ) decreases with increasing the Al-doses; e.g., Λ = 0.42520 nm for as-deposited TiN and Λ = 0.42253 nm for TiN with an Al-dose of 4.5 x 10^{17} ions/cm^2, as listed in Table 1. No significant change in the lattice constant was observed when the Al-dose exceeded 2.9 x 10^{17} ions/cm^2. The residual stress is estimated from the measured difference of lattice parameters and the elastic constants. As also listed in Table 1, the residual stress varies with the Al-doses from the tensile state for the as-deposited TiN to the compressive one in all the Al-implanted TiN films. The residual stress becomes more compressive with increasing ion

momentum or Al-doses. In [37], the effect of atom peening on this substitution of titanium atoms by aluminum one drives the forward momentum of the ions to the TiN lattice. This effect results in the build-up of dislocations and induces the compressive stresses below the surface and/or a refinement of microstructure.

Table 1 Variation of the lattice parameter and residual stress with increasing the aluminum doses in the aluminum implantation to as-deposited TiN.

Material	**Lattice Constant**	**Residual Stress**
As-deposited TiN	0.42520 nm	+1.02 GPa
TiN + 1.0 x 10^{17} Al/cm^2	0.42275 nm	-1.40 GPa
TiN + 2.9 x 10^{17} Al/cm^2	0.42253 nm	-1.62 GPa
TiN + 4.5 x 10^{17} Al/cm^2	0.42250 nm	-1.65 GPa

To be noticed in [38–40], the residual stress state is sensitive to the processing conditions in PVD/CVD. The bias voltage in spattering or the increase of physical bombardment promotes higher intrinsic stresses in the coating. In particular, an optimization of processing conditions is often necessary to induce higher residual stresses into the PVD coating.

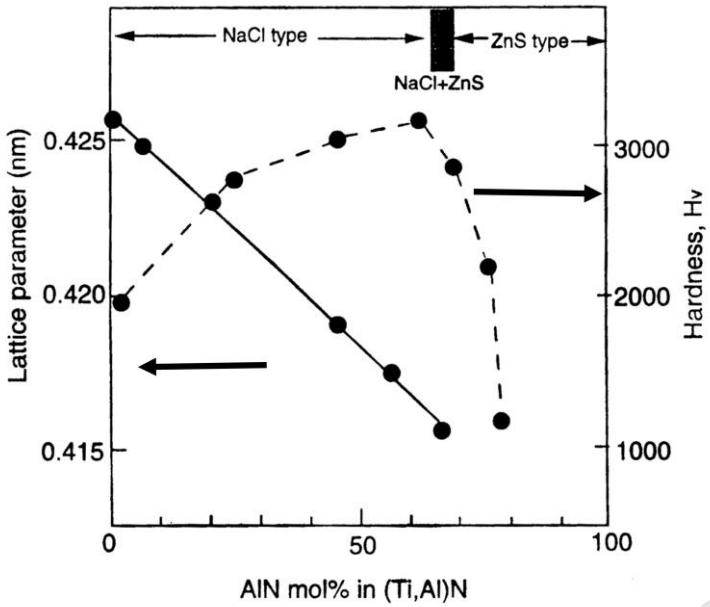

Fig. 7 Variation of the lattice parameter and the residual stress with increasing the molar ratio of AlN in the solid solution of (Ti, Al) N.

Variation of the residual stress with increasing the Al-dose in Table 1 is reconsidered from the transformation in the AlN-TiN system. The original TiN lattice releases its residual stress by precipitation of a new metastable phase of (Ti, Al) N. The cubic-AlN phase predominates up to x = 0.6 and for Al fractions beyond 65%. The wurtzite phase is selected as depicted in Fig. 7. A decrease in the TiN unit cell dimension is caused by the substitutional replacement of the Ti-sublattice by Al-atoms due to the kick-off mechanism. The linear decrease of the lattice constant with increasing the AlN molar ratio reveals that a solid solution of AlN takes place in TiN in this alloying. Owing to this solid solution, the hardness increases monotonously with increasing Al-dose. This increase in hardness implies that the wear toughness is promoted by increasing the hardness-to-Young's modulus ratio (H/E) through this alloying.

This section focuses on the oxidation behavior of the binary nitride (Ti, Al) N. Figure 8 shows the variation of measured mass gain with the duration time in the oxidation test under the

oxygen atmosphere at the temperatures of 600˚C, 700˚C, and 800˚C, respectively. Little mass gain is detected even after the oxidation test for 20 h at 600˚C. The oxidation toughness is significantly improved by this formation of (Ti, Al) N. In a similar manner to Section 2.2, the activation energy is estimated for this Al-implanted TiN by the Al-dose of 4.5 x 10^{17} ions/cm^2. Since E_a = 364 kJ/mol, twice more than E_a for as-deposited TiN, this (Ti, Al) N has sufficient oxidation toughness in practice. This significant increase in E_a comes from the microstructure evolution during oxidation. At 700˚C, the parabolic evolution of mass gain is retarded in comparison to the mass gains in Fig. 6. To be noticed, this slow evolution changes to rapid growth of oxidation around 700 mins at 800˚C. At this change, the crack penetrates through (Ti, Al) N coating matrix so that more volume of (Ti, Al) N is subjected to oxidation.

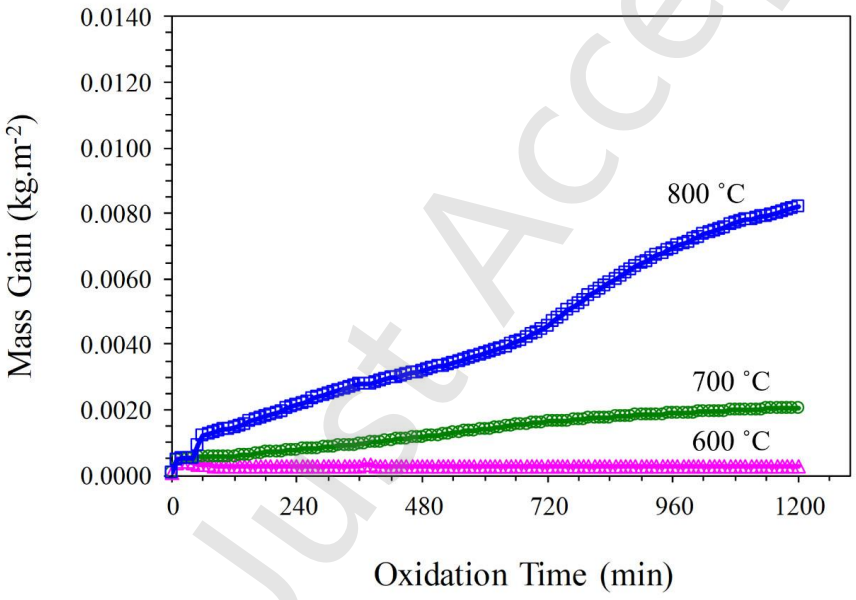

Fig. 8 Time evolution of the mass gain for the Al-implanted TiN coatings with the dose of 4.5 x 1017 ions/cm^2 at the holding temperatures of 600˚C, 700˚C, and 800˚C.

As precisely analyzed by X-ray Photoelectron Spectroscopy (XPS) in [17,19], the bound aluminum in (Ti, Al) N and the unbound aluminum atoms diffuse to the surface against the oxygen atom penetrating from the surface to the depth of (Ti, Al) N. Due to the direct reaction between the

penetrating oxygen and diffusing aluminum, an aluminum oxide is synthesized to form the protective layer on the surface. Figure 9 depicts the cross-sectional image of (Ti, Al) N after an oxidation test for 20 h at 600˚C. A dense α-Al_2O_3 layer is formed on the surface to prevent the matrix in depth from further oxidation. This in situ formation of a protective layer of dense corundum α-Al_2O_3 structure blocks further oxygen diffusion and suppresses the mass gain of (Ti, Al) N coating during the oxidation wear. This self-protection mechanism and high H/E ratio prolong the (Ti, Al) N coated tool life even during the hot metal forming.

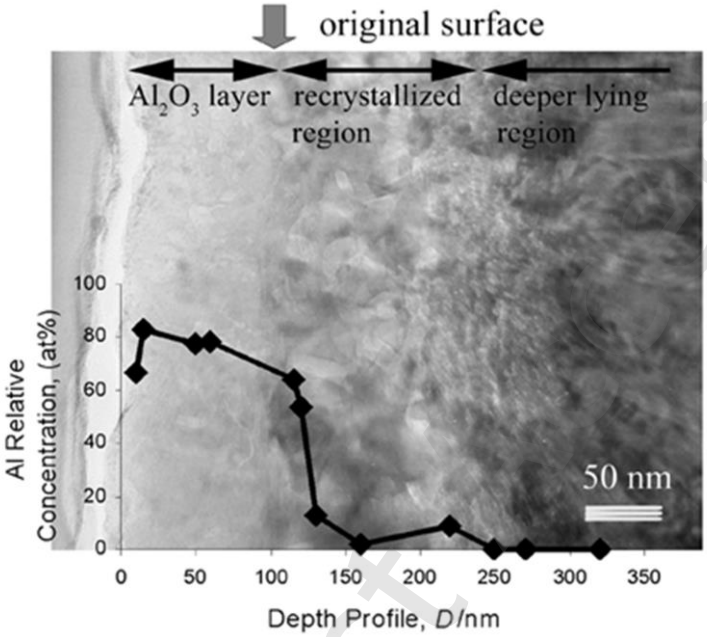

Fig. 9 Formation of nano-crystalline, dense a-Al_2O_3 layer on the surface after oxidation testing at 600˚C for 20 h. Diffusing aluminum atoms from the coating reacted with oxygen atoms to form the stable oxide surface layer to block the further oxidation process from the surface to the depth.

As pointed out in [17,19], this in situ-formed corundum layer has sufficient toughness during the higher temperature transients above 1,000˚C for 1.8 ks. This layer only breaks away partially after a long duration at this high temperature. These experimental data suggest that 1. basic monolithic nitride system must be selected to increase the oxidation wear toughness in higher

temperature, 2. dissociation mechanism of bound aluminum in the binary nitride system is rate-dependent and must be controlled against the accelerated oxygen diffusion from the surface at the elevated temperature, and 3. the diffusion distance for dissociated, unbound aluminum is designed to be short enough to easily form the dense corundum sublayers in the coating. In the following, these first two items are considered by discussing the binary nitride coating recipe to compare the (Ti, Al) N (or TiAlN) and (Cr, Al) N (or CrAlN). The third item is reconsidered in the multi-layered and nano-laminated binary nitride coatings.

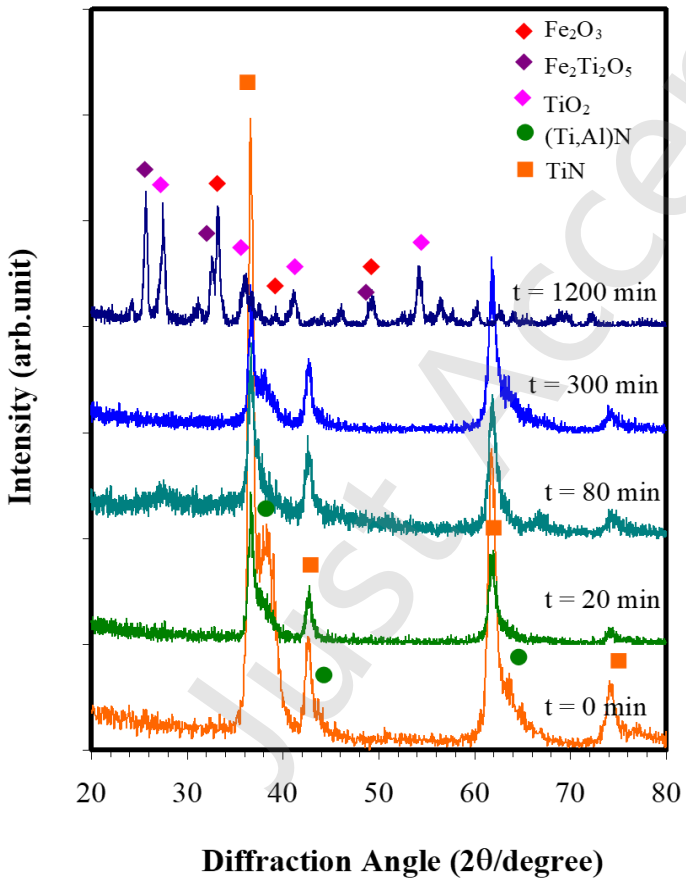

Fig. 10 Variation of the XRD diagrams for oxidized Ti(Al)N coatings with increasing the oxidation time.

An oxidation test was performed at 800˚C to investigate the kinetics of oxide formation in the Ti(Al)N coating system. Figure 10 compares the XRD diagrams of oxidized Ti(Al)N coating with increasing oxidation time. In the case of the monolithic TiN coating, the titanium oxide peaks were detected in the early stage of testing. None of the TiO_2 or Fe_2O_3 peaks were seen at 800˚C for 5 h. The peaks corresponding to TiN and (Ti,Al)N disappeared progressively when increasing the time to over 15 h. Several peaks of TiO_2, $Fe_2Ti_2O_5$, and Fe_2O_3 appear instead of the original nitrides when increasing the time up to 20 h. This abrupt change corresponds to the breakage of the protective a-Al_2O_3 layer in Fig. 9.

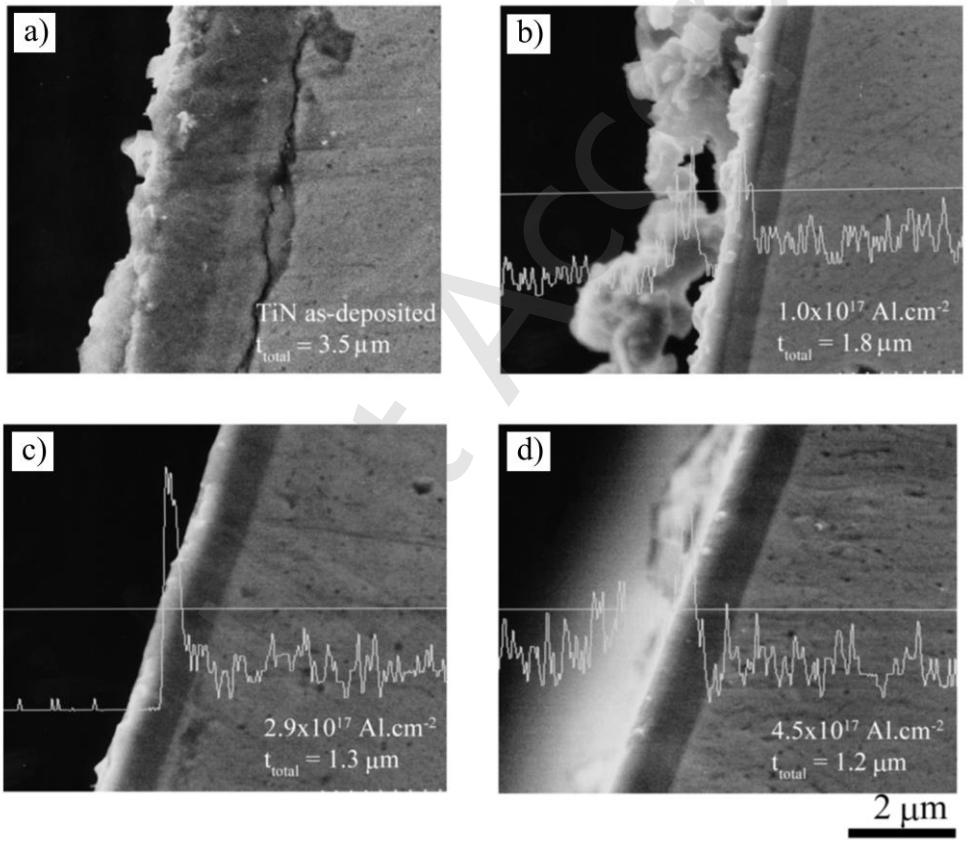

Fig. 11 Total oxidized layer thickness and aluminum line profile from rapid oxidation testing of four specimens (TiN and Ti(Al)N with different aluminum contents) at 1,000˚C: a) TiN as deposited, b) 1.0 x 10^{17}Al.cm^{-2}, c) 2.9 x 10^{17} Al.cm^{-2}, and d) 4.5 x 10^{17} Al.cm^{-2}

A rapid oxidation test at 1,000˚C was performed to describe the oxidation toughness of Ti(Al)N with different Al contents. The oxidizing temperature was continuously increased from room temperature to 1,000˚C without any soaking time. Four different specimens were prepared for the measurement of the oxidized layer thickness on the cross-sectional SEM images, as shown in Fig. 11. The monolithic TiN film was rapidly oxidized to form a mixed oxide scale. The total layer thickness is twice thicker than the initial one (1.2 μm). The oxide scale grew outward and expanded. It seems to be broken away or to delaminate from the substrate. In contrast, the Al-implanted TiN or Ti(Al)N coatings showed less change in the total thickness with increasing Al contents. The aluminum line profile observed by EDS was also superimposed onto the SEM image from the film surface to the stainless-steel substrate. Little change of aluminum profile proves that Ti(Al)N coating has less volume expansion as well as higher oxidation resistance than the monolithic TiN. The surface morphological changes observed by SEM micrographs of oxidized specimens revealed that various surface oxide scales were formed on the films after high thermal test 1,000˚C at heating rate 1 ˚C.min^{-1} without soaking time, for TiN and Ti(Al)N with 1.0 x 10^{17}, and 2.9 x 10^{17} Al.cm^{-2}. With EDS analysis, TiN was oxidized to TiO_2 and spinel oxides on the surface. A smooth scale was homogeneously formed on the surface of Ti(Al)N film with 2.9 x 10^{17} Al.cm^{-2}. No scales were seen on the surface of Ti(Al)N film with 4.5 x 10^{17} Al.cm^{-2}. These results indicate that increasing Al content enhances oxidation resistance and mitigates oxidation-induced stresses, thereby improving the structural integrity and effective high-temperature toughness of binary Ti(Al)N coatings. Although direct fracture toughness values are not widely reported in the literature for these systems, resistance to oxidation-induced cracking and delamination can be considered an indirect indicator of coating toughness under high-temperature service conditions.

2.4 Binary Nitride Coating Design for Hot Metal Forming

In the binary nitride coating design, aluminum is selected as a constituent element for the self-protection of base monolithic nitride coatings, such as TiN and CrN, under hot metal forming conditions. The design concept is described in terms of the friction coefficient measured by the BOD test and the holding temperature. As compared in Fig. 12, PVD TiN coating is available in the temperature range below 500˚C. As stated in Section 2.2, its tribological behavior is characterized by relatively high friction around $\mu = 0.6 \sim 0.7$ under high loading conditions. Through the solid solution of carbon into the TiN, the friction coefficient is reduced to $\mu = 0.25 \sim 0.35$, but heat resistance is not improved. As pointed out in Section 2.3, TiAlN has higher oxidation toughness than TiN. This binary nitride coating works in the hot metal forming below 900˚C. Owing to the aluminum solid solution in TiN, the hardness is increased from 1800 HV for TiN to 2800 HV in commercial. The friction coefficient slightly decreases compared to TiN.

CrN coating has a slightly lower hardness of 1600 HV than TiN. Its working temperature is promoted to be from 500˚C to 700˚C. This higher heat resistance is preferable as a protective coating of parts and tools under severe conditions with hot spots. Aluminum solid solution to this CrN also promotes oxidation toughness. CrAlN coating works even in the range from 900˚C to 1,100˚C with nearly the same friction coefficient as CrN. Hence, this CrAlN is expected to work at the hot forging with local hot spots.

However, it should be emphasized that the friction coefficients obtained from BOD tests in Fig. 10 are primarily used to illustrate general temperature-dependent trends and to support the conceptual design framework of nitride coatings. In BOD testing, the contact conditions, such as normal load, sliding speed, and temperature, are typically maintained constant, allowing steady-state friction values to be obtained. In contrast, industrial hot forming processes involve highly transient thermo-mechanical conditions, where contact pressure, sliding velocity, and interfacial temperature continuously evolve during deformation. Under such transient conditions, the tribological performance of the coating may deviate from steady-state laboratory results due to changes in

transfer layer formation and thermo-mechanical conditions. It is well recognized that tribological behavior is dependent upon the entire tribological system, including the workpiece material, coating composition and structure, lubrication condition, and evolving contact parameters. Therefore, while BOD testing provides valuable comparative insight under controlled conditions, its results should be complemented with specific tribometers for metal forming, as discussed in Section 3.

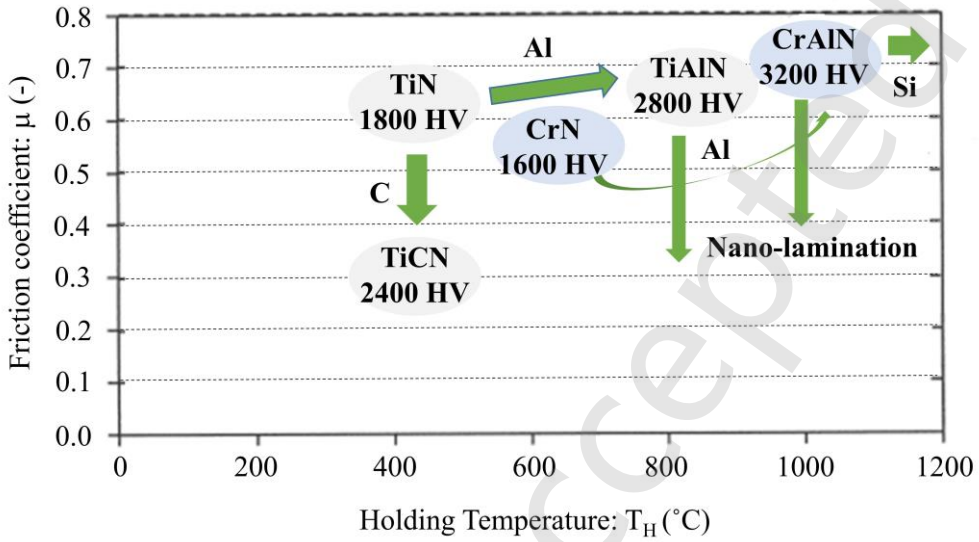

Fig. 12 Feasibility of PVD monolithic and binary nitride coatings in the function of the friction coefficient and the holding temperature.

Ternary and quaternary alloying stand on these characteristics of binary nitride coating in Fig. 12. A refractory metal element, such as Si, Zr, or Co, becomes a candidate as the third and fourth cations in the alloying system. Next, selecting the cation element in those binary, ternary, and quaternary alloying is considered.

In the coating design of protective coating for hot metal forming, the stability of in situ formed metallic oxides must be taken into account. After the classical treatise in [41], the metal-to-oxide volume ratio or the Pilling-Bedworth Ratio (R_{PB}) works as a critical parameter to describe the stability of in situ formed oxide layer during the hot metal forming. As proved in [42], the oxide film with $R_{PB} < 1$ is too thin to sustain the role of a protective layer. When $R_{PB} > 2$, the oxide layer chips

off and does not prevent the coating matrix from further oxidation. Only when $1 < R_{PB} < 2$, the oxide layer has the capacity to work as a protective layer without cracks. Table 2 summarizes the metal-to-oxide volume ratio or R_{PB} for various kinds of metals as a cation in nitrides. Aluminum, zirconium, hafnium, titanium, iron, platinum, and chromium are typical metallic elements to satisfy $1 < R_{PB} < 2$. However, even in those metal-to-oxide systems, their capacity for protection against oxidation is strongly dependent on their growth mechanism as well as the coating structure. Titanium and iron atoms diffuse to the surface against the oxygen atom penetrating from the surface. Under this co-diffusion process, their oxides are formed in the coating matrix with a rate dependency. In the case of aluminum and zirconium, their stable oxide layers are in situ formed as a protective layer against further oxidation. Other cation elements than Al and Zr, such as Si and V, are considered as candidate cations in the multi-layered or the nano-laminated coating system.

Table 2 A list of metal oxides with oxide-to-metal volume ratio after the Pilling and Bedworth principle.

Oxide	**Oxide-to-metal volume ratio**
MgO	0.81
Na_2O	0.97
Al_2O_3	1.28
ZrO_2	1.56
NiO	1.65
FeO	1.68
TiO_2	1.70 - 1.78
CoO	1.86
Cr_2O_3	2.07
Fe_2O_3	2.14
Ta_2O_5	2.50

Nb_2O_5	2.68
V_2O_5	3.19
WO_3	3.30

Based on alloying element design against oxidation wear, the utilization of these two binary nitride systems as protective coatings for dies and tools in hot metal forming can be summarized. As depicted in Fig. 13, this recipe consists of several categories and directions. Ti-based coating systems, such as TiN and TiCN, are available in metal forming with highly applied stress transients at lower temperatures than 427˚C with less formation of titanium oxides. Above 427˚C, the formation and growth of TiO_2 is accompanied by fatal cracking in the coating system. In the temperature range below 727˚C, TiAlN is responsible for fine protection of dies and tools. The applied stress has a significant influence on the coated die life in that temperature range. Hence, its practical feasibility must be checked in each application. In particular, the hot deformation and creep straining commence in heat-resistant steel dies above 627˚C. The maximum stress applied to these TiAlN-coated dies must be lower than the critical stress, which is expected to drive significant time-dependent strains. CrAlN might be utilized for hot metal forming above 677˚C. When applied stress is reduced enough to suppress the oxidation wear as well as the hot deformation of substrates, this heat-resistant coating is useful below 1,000˚C.

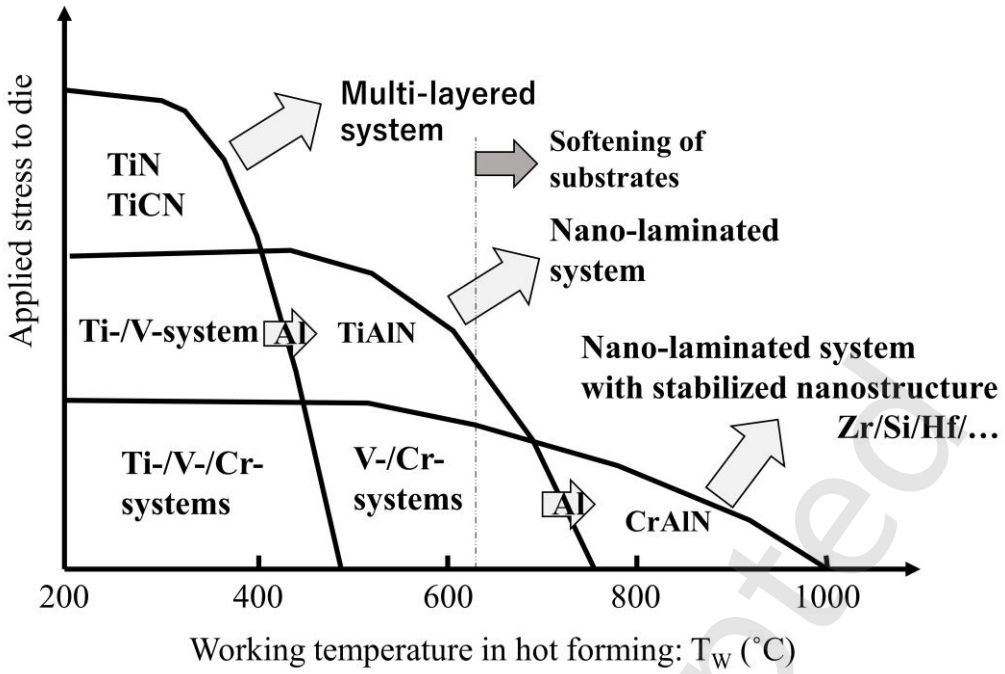

Fig. 13 Recipe on how to use TiAlN and CrAlN systems as a protective coating for the hot metal forming dies.

A multi-layered TiN-based coating is available to extend the critical stress limit below 400˚C [43]. To be discussed later, fatal delamination is prevented by no occurrence of penetrating cracks through the thickness of the multi-layered coating system. In order to extend the TiAlN-coated die life in the working temperature range between 400˚C and 600˚C, nano-lamination is effective in practice [44]. The life of CrAlN-coated dies is also expected to be prolonged by the nano-lamination of two CrAlN-based sublayers with the bilayer thickness less than 10 nm [45]. The critical stress is suppressed by the micro-cracking on the alternative interfaces in the nano-laminated coating system. In order to promote the heat resistance above 1,000˚C, this nano-lamination had better accompany the stabilization of tailored nanostructures [46].

In short, the improved performance of nitride coatings in hot metal forming arises from the synergistic interaction among multiple alloying elements rather than from a single constituent. Aluminum primarily contributes to the formation of stable and protective oxide layers, while

chromium enhances thermal stability and resistance to adhesion. Additional alloying elements, such as Si or Zr, may further stabilize the microstructure through nanostructural refinement or oxide-scale control. The combined effects of solid-solution strengthening, controlled oxide formation, and structural stabilization determine the durability of multicomponent nitride coatings under severe thermo-mechanical conditions.

2.5 Improvement of Tribological Characteristics by Laminated Coating

The multi-layered and nano-laminated coating systems provide another direction to make full use of monolithic and binary nitride coatings. The multi-layered coating approach has been widely utilized in industries as a laminated composite of several film sublayers with different alloying elements [47]. In particular, a protective coating for cutting tools has a composite structure with four to five sublayers [48]; e.g., a coated end-milling tool by TiAlN, Al_2O_3, nano-diamond layer, and so forth.

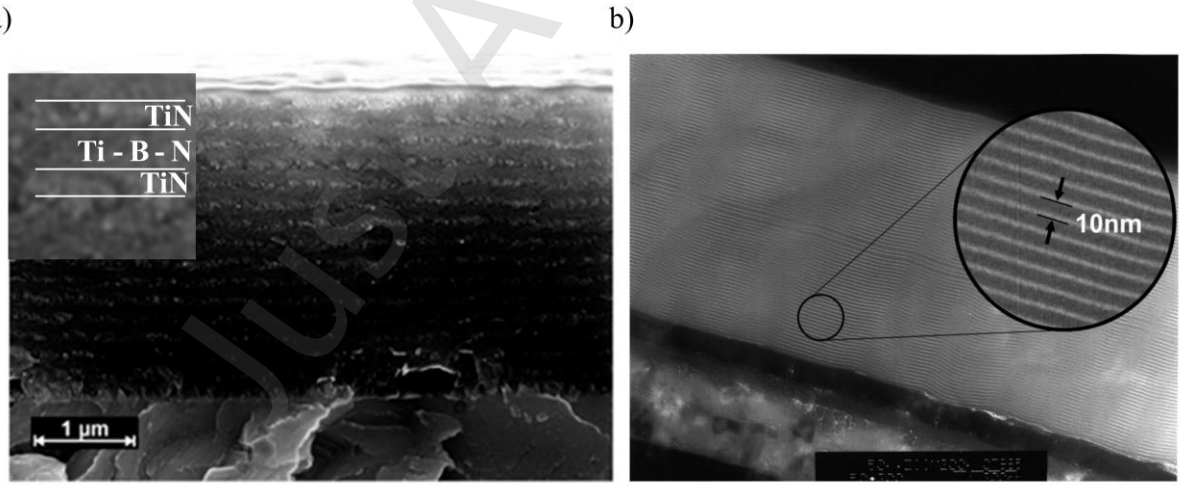

Fig. 14 Nano-scale multi-layered coating: a) Nanolaminated coating of dissimilar sublayers by TiN/Ti-B-N, and b) Nanolaminated coating of similar DLC sublayers with different mass densities.

In this selection, the effect of the nanolayered structure on the mechanical properties and tribological performance is pointed out. There are two schemes in PVD to construct the nano-

laminated coating system. In the former, two dissimilar sublayers are stacked alternatively into a nanolayered coating. For example, TiN and Ti-N-B sublayers with the specified film thickness were alternatively stacked into a nanolayered coating [49], as depicted in Fig. 14a. Then, two similar sublayers with different mass densities or cluster nanostructures were also stacked alternatively to a nanolaminated coating. The amorphous carbon sublayers with different mass densities were nanolaminated into a coating [50], as shown in Fig. 14b. The multi-layered coating has comparable mechanical properties to each sublayer film until the bilayer thickness is much more than 10 nm. With increasing the number of layers in a coated film, or with decreasing the bilayer thickness, the mechanical properties of the nanolaminated film exceed those of each constituent sublayer film. Figure 15a depicts the variation of hardness (H_{nano}) and elastic modulus (E_{nano}) of nanolaminated TiN/Ti-N-B films with increasing the number of laminates. When the bilayer thickness is in a submicron scale, E_{nano} is less than E_{TiN}, and H_{nano} is less than $H_{Ti\text{-}N\text{-}B}$. When the bilayer thickness approaches 10 nm, these exceed E_{TiN} and $H_{Ti\text{-}N\text{-}B}$, respectively. After the micromechanical treatise on the mechanical properties of the composite materials [51], these mechanical properties of nanolaminated TiN/Ti-N-B film must satisfy that $E_{Ti\text{-}N\text{-}B} < E_{nano} < E_{TiN}$ and $H_{TiN} < H_{nano} < H_{Ti\text{-}N\text{-}B}$. Figure 13a proves that $E_{nano} > E_{TiN} > E_{Ti\text{-}N\text{-}B}$ and $H_{nano} > H_{Ti\text{-}N\text{-}B} > H_{TiN}$. This reveals that the nanolaminated film is never a composite of constituent sublayers but that the nanolaminated structure of dissimilar sublayers has a significant influence on its mechanical properties.

a)

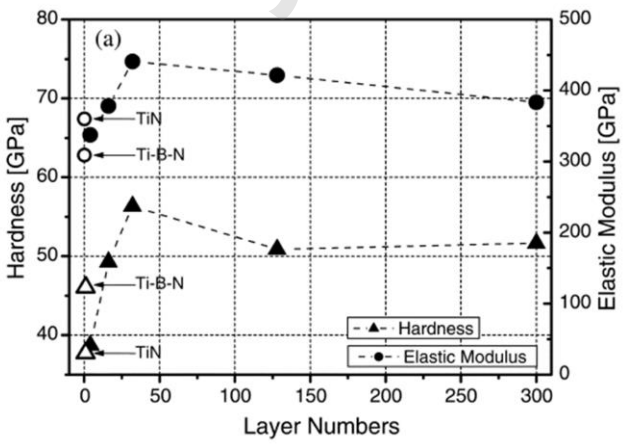

b)

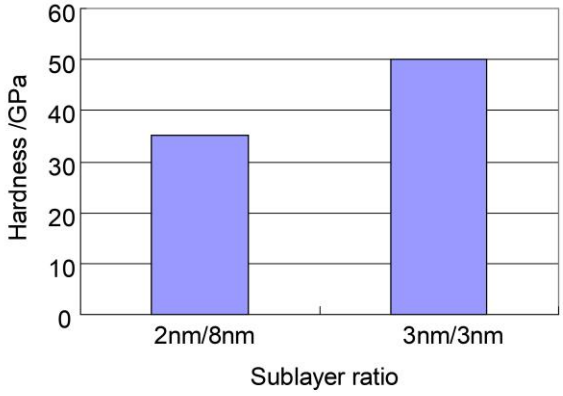

Fig. 15 Effect of the nanolamination to the mechanical properties of nanolaminated films: a) Variation of elastic modulus and hardness of dissimilar nanolaminated films with increasing the number of layers in the system of TiN/Ti-B-N, and b) Effect of sublayer ratio in the nanolamination of similar sublayers with different mass densities on the hardness.

To be noticed, this effect on the mechanical properties is not only adaptive to the nanolaminated system of dissimilar sublayers in Fig. 14a but also true to the nanolaminated system of similar sublayers with different mass densities in Fig. 14b. Figure 15b compares the measured hardness of nanolaminated DLC films with different sublayer thicknesses [52]. The difference in hardness proves that the nanolaminated structure itself promotes the elastic modulus and the hardness of nanolaminated films. Figure 14 also suggests that the interface of nanolaminated sublayers plays a role in strengthening and toughening the total coating system.

The effect of nanolamination on the tribological performance of nano-scale multi-layered coatings is considered in this selection. Two types of wear experiments were employed to describe the wear-induced failure and abrasive wear of the nanolaminated coating. First, the hard ball impact experiment was utilized to evaluate the breaking failure with increasing the number of impact shots (N). In general, the incremental damage by impact loading advances to fatal failure of the coating since an induced small-scale crack grows to be a penetrating crack through the film thickness [50]. A hard ball with a diameter of 5 mm was shot onto the coated specimen, which was placed with a skew angle of 15^{o} to the support. The dynamic load and the total TiAlN film thickness were constant at 200 N and 6 μm, respectively. As shown in Fig. 16a, the coating failed area monotonically increases with increasing the number of impact shots in the mono-layered TiAlN coating. Then, the fatal failure of coating by the penetrating crack occurs at the critical number of impact shots around 3 - 5 x 10^{5} shots when extrapolating the data in Fig. 16a. On the other hand, when using the nanolaminated coating by TiN/TiAlN, the onset of visible initial cracking is retarded from N = 1 x

10^4 shots to 3.6 x 10^4 shots. The crack growth rate was nearly arrested when N > 1.0 x 10^5 shots. No fatal failure occurs when using the nanolaminated coating. This crack arresting process by nanolamination of coating comes from the micro-cracking toughness on the interfaces of nanolaminates. After the fracture mechanics of the interface-strengthened composite materials [53], the lateral cracking mode along the interface is selected more easily than the penetrating crack mode across the interface. This implies that a penetrating crack encounters the nanolaminate interface and branches to a lateral cracking along the nanolaminate interfaces. The nanolaminated coating itself is prevented from the fatal fracture or complete delamination.

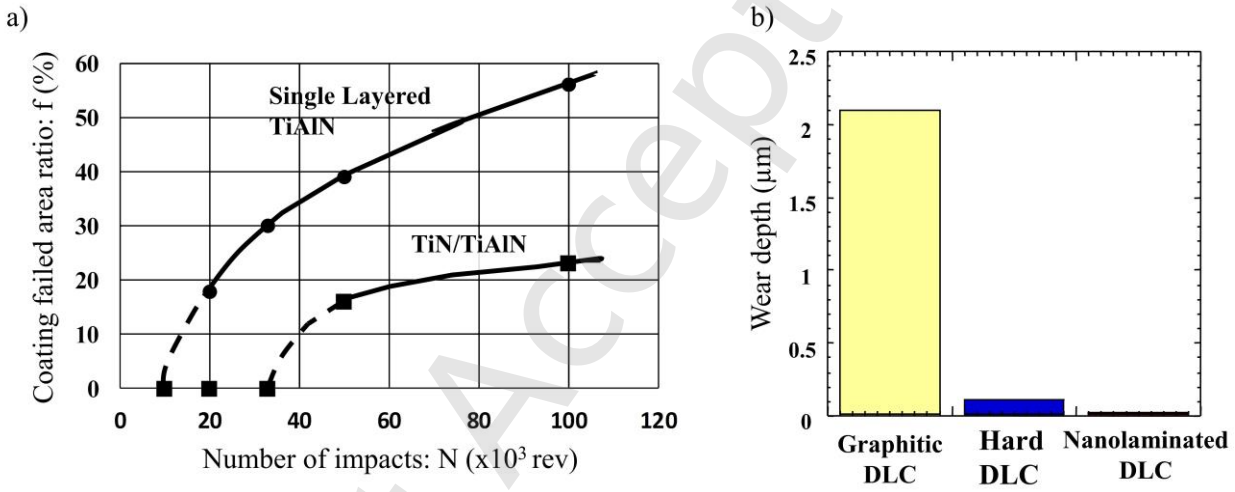

Fig. 16 Tribological performance on the nanolaminated coating of dissimilar and similar nanolayers in the wearing experiments: a) Variation of the crack-failed area ratio with increasing the number of impact shots in the nanolaminated coating of TiN/TiAlN system, and b) Comparison of the worn depth of coated films among the graphitic DLC, the hard DLC, and the nanolaminated DLC with different mass densities.

The nanolamination effect on the wearing behavior in the above is further discussed in the abrasive wearing experiment of the nanolaminated coating of similar nanolayers with different mass densities. Three DLC coatings were employed for the abrasive wearing experiment, where the alumina ball with a size of 30 μm was shot at the incident angle of 30° to the coated specimen at the

pressure of 5 kg/cm^2 by the accelerated flow rate of 150 l/min. The abrasively worn depth of coating is compared among the graphitic DLC, the hard DLC, and the nanolaminated DLC with different mass densities. As shown in Fig. 16b, the worn depths are experienced in the former two coatings, but they approach nearly zero in the nanolaminated DLC coating. This teaches that no significant abrasive wear takes place even in the nanolaminated coating of similar nanolayers with different mass densities. These two wear experiments prove that a nano-scale multi-layered coating system provides a method to be free from total failure and wear-induced deterioration of the coating.

The selection of the alloying element is also important to design each nanolayer system and interface. As discussed before, a nanolaminated system of monolithic nitride sublayers, such as TiN/Ti-B-N, TiN/CrN, and so forth, has low oxidation wear toughness at elevated temperatures. Each nanolayer with the lowest oxidation toughness changes itself to oxides as a starter of cracking. When using the binary and ternary nitride films as a constituent nanolayer, the cation atoms must be selected with consideration of the nucleation and growth of oxides during hot metal forming. Vanadium was often used as a substitutional element of aluminum in the binary nitride coating design [54]. Silicon was also employed to strengthen and toughen TiN by the formation of a nano-composite TiSiN coating, instead of aluminum [55]. In the nanolayered coating design, this silicon selection was important to increase the total wear toughness even in the severe wearing conditions by nanolamination of CrAlN/TiSiN [56].

3 Applications of Nitride Coating to Hot Metal Forming Dies

As noted in the introduction, dies in metal forming processes are typically subjected to severe contact loads. To extend their service life, die materials are required to have better wear and seizure resistance. At the same time, environmentally friendly approaches, such as semi-dry and dry processes in which the surface coatings and other surface treatments replace conventional lubricants, have become increasingly important [57]. Accordingly, this section describes representative

applications of nitride coatings used in the hot forming of steels, aluminum alloys, magnesium alloys, and titanium alloys.

3.1 Hot Forming of Steels

Over the past 15 years, ultra-high tensile steel (UHSS) and aluminum alloys have been increasingly used in the transportation sector, particularly in the automotive industry, where weight reduction and crashworthiness are critical requirements. As shown in Fig. 17, the strength of steel sheets used for car body frames has steadily increased [58]. UHSS, in particular, is a significant material development and is now employed with a strength of up to 1,300 MPa, leading to hot forming indispensable. Under such demanding conditions, the forming load increases, while the formability decreases. Thus, the durability and lubricity of the dies are increasingly required. Consequently, enhancing the tribological properties of dies at elevated temperatures has become essential.

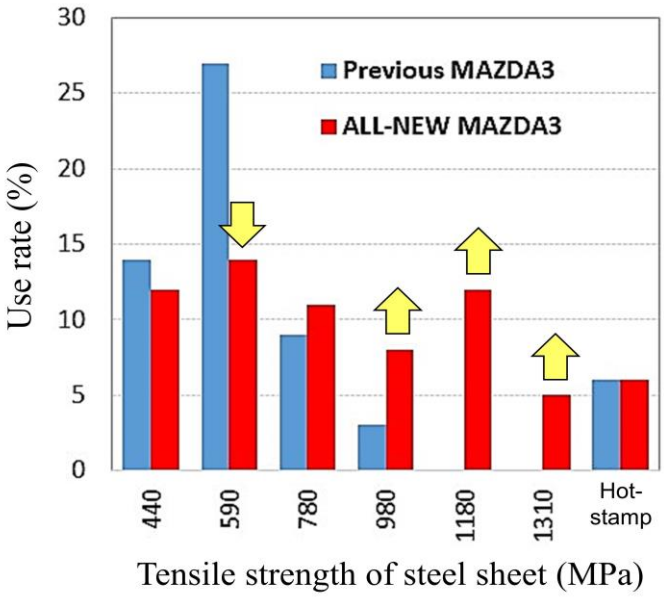

Fig. 17 Steel sheets of the new Mazda 3 [58].

To evaluate the tribological properties of forming tools used with steels, including UHSS, a high-frequency linear oscillation ball-on-plate test (SRV-type test) was employed as a sliding friction test. In this study, the tools were uncoated and coated with TiN, CrN, and AlCrN. Additionally, AlCrN had two different hardness levels: 26 and 32 GPa. They were against SUJ2 steel balls at room temperature [59]. Figure 18 compares the specific wear of uncoated, TiN, CrN, and AlCrN. It was found that the CrN coating had the highest wear resistance. Furthermore, the elemental analysis of CrN and AlCrN was conducted. Figure 19 shows that iron oxide (FeO) adhered to the sliding surfaces of both CrN and AlCrN. Nonetheless, the amount of FeO on the AlCrN was less than on the CrN. This is attributed to the presence of aluminum, which reduces adhesion tendency when compared to chromium. Based on these findings, the AlCrN, which demonstrated superior wear and adhesion resistance, was further investigated in deep drawing tests on UHSS to simulate actual forming conditions under a contact pressure of 1.2 GPa. As shown in Fig. 20, the higher hardness AlCrN exhibited significantly greater wear resistance than the lower hardness AlCrN.

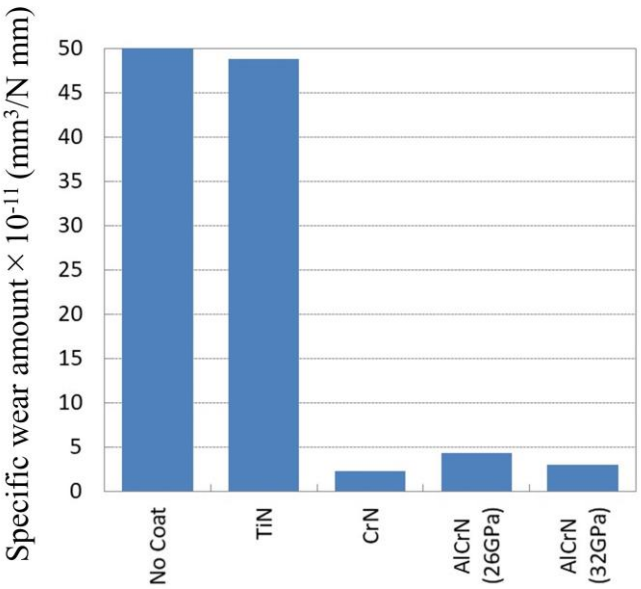

Fig. 18 Specific wear amount of various PVD coatings from the SRV-type test [59].

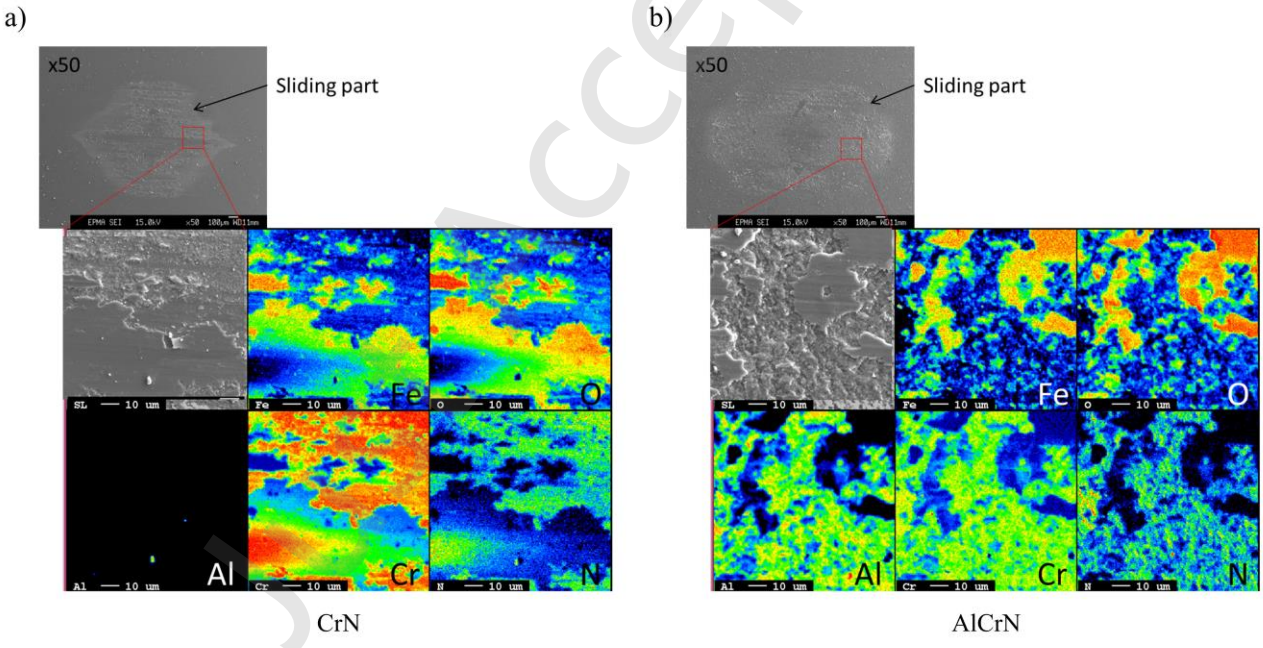

Fig. 19 Elemental analysis on the sliding surfaces after the SRV-type test: a) CrN and b) AlCrN [59].

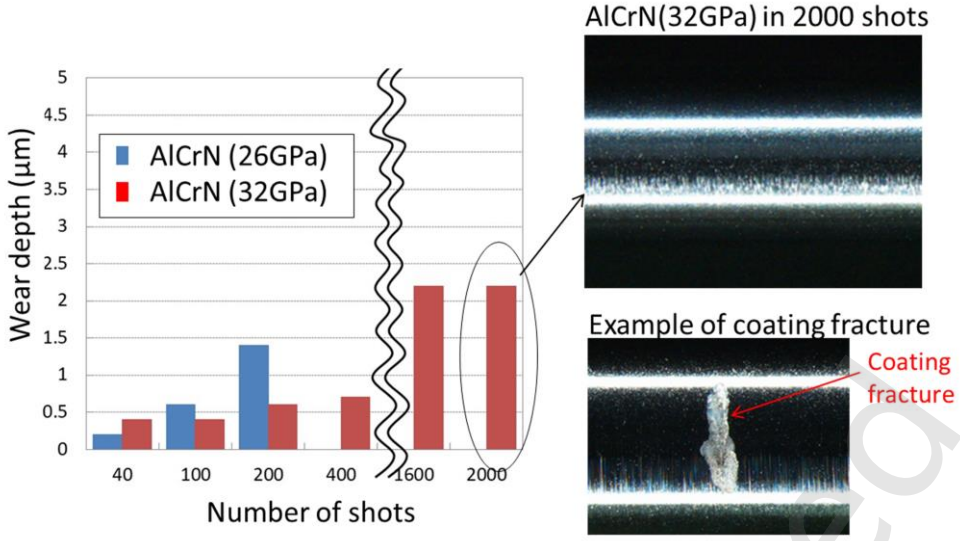

Fig. 20 Wear depth versus number of shots in the deep drawing test of UHSS [59].

In general, Al-Si or Zn coatings are coated on the workpiece for high-strength materials, such as UHSS, to mitigate oxidation at high temperatures and to reduce tool wear [60–64]. Strip-type friction tests, as illustrated in Fig. 21, are typically applied as a tribometer to evaluate friction and wear in sheet metal forming [65]. Prakash et al. conducted a series of studies [66–68] by using the hot strip drawing test to investigate the friction coefficient and tool wear in the hot stamping of 22MnB5 steel. In those studies, the workpieces were coated with Al-Si and uncoated, while the tools were uncoated and coated with AlCrN and CrWN. Figure 22 presents the conclusions in a schematic diagram of tool-workpiece adhesion. Applying the Al–Si coating to the workpiece could enhance the wear resistance of the tool by two times or more, while applying the PVD coatings to the tools could reduce wear up to ten times, regardless of whether the workpiece was coated.

In particular, AlCrN and CrWN provided significant improvements in wear resistance. However, a critical issue in these systems is the adhesion of the Al–Si layer from the workpiece to the tool surface. The role of Al in CrN-based coatings was also reported: 3D optical interferometry revealed more Al–Si adhesion on AlCrN-coated tools when compared to CrWN-coated tools. The difference came from the addition of W to CrN. It increases tool hardness as well as decreases

chemical affinity to aluminum. Additionally, the influence of the nitriding layer in the pretreatment is also significant in reducing adhesion and galling since the nitriding layer causes the bonding between the substrate and the coating. Therefore, both coating composition and nitriding layer thickness must be carefully considered in coating design.

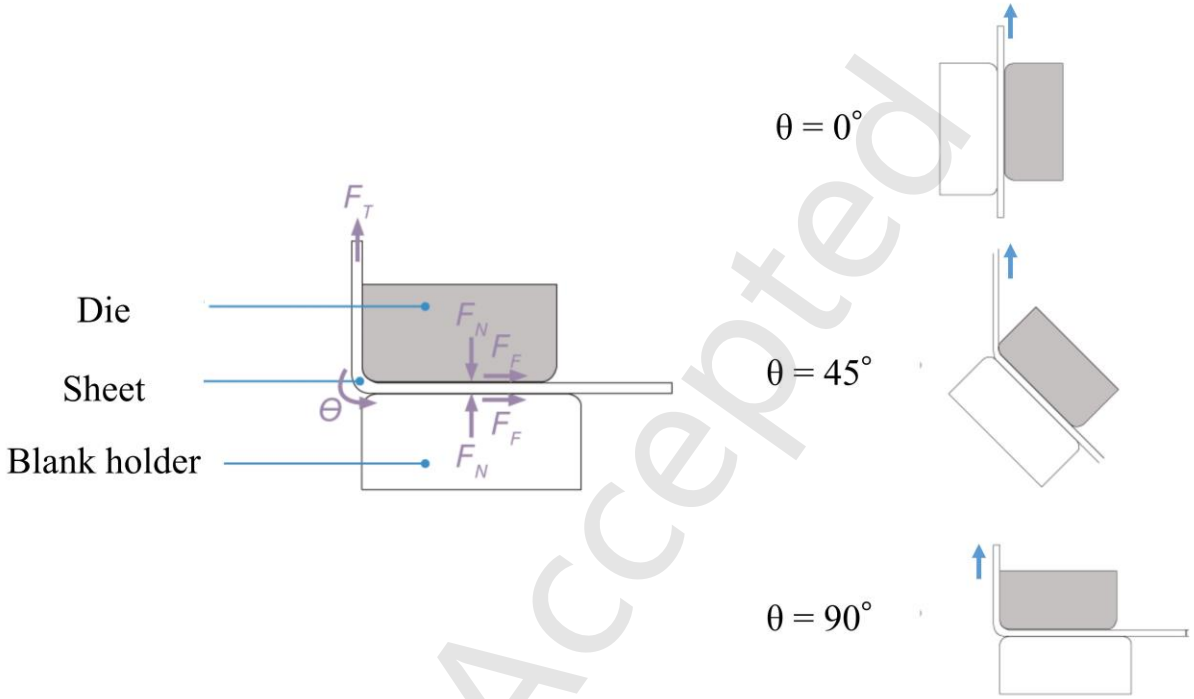

Fig. 21 Schematic of the hot strip drawing test with different configurations [65].

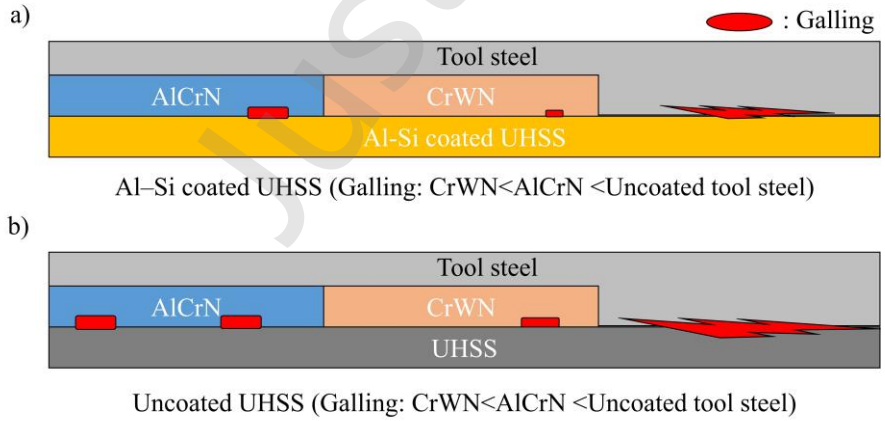

Fig. 22 Schematic diagram of tool and workpiece adhesion: a) Al–Si coated UHSS, and b) Uncoated UHSS [66–68].

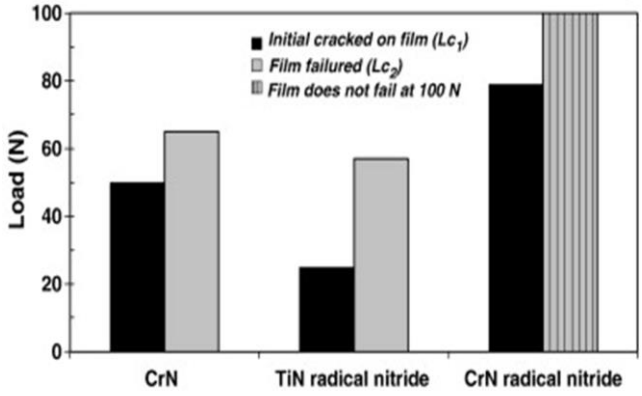

Fig. 23 Scratch test results of each surface condition [69].

To study the effect of nitriding, Sresomroeng et al. [69] applied the radical nitriding as a pretreatment for CrN and TiN coatings. As compared in Figure 23, scratch tests confirmed that the radical nitrided layer enhanced the bonding strength of the CrN films when compared to the non-nitrided coating. For more information, the deep drawing of advanced high strength steel (AHSS) was also conducted to evaluate its tribological properties. The result found that the CrN coating with the radical nitriding could maintain the surface integrity up to 1,000 strokes, whereas the conventional CrN film showed peeling and increased surface roughness. This finding indicates that the radical nitriding before coating significantly improved adhesion resistance and extends the service life of the dies in AHSS forming.

In warm and hot forging, Dubar et al. [70–72] investigated tribological phenomena by using the Warm and Hot Upsetting Sliding Test (WHUST). This test can conduct severe contact conditions and perform experiments at temperatures above 1,000°C. Figure 24 compares the adhesion of AISI 304 stainless steel against AISI H11 hot tool steel evaluated at 1,100°C. In this study, there were three tool conditions: alumina sol-gel coated tools loaded with an alpha alumina coating, alumina sol-gel coated tools loaded with a hexagonal boron nitride coating, and uncoated tools. The results found that the alumina sol-gel coated tool exhibited better adhesion resistance when compared to the

uncoated tool, particularly at temperatures above 1,000 °C. In particular, the alumina sol-gel coated tools loaded with hexagonal boron nitride coating provide a low friction coefficient and good compatibility with graphite lubricant.

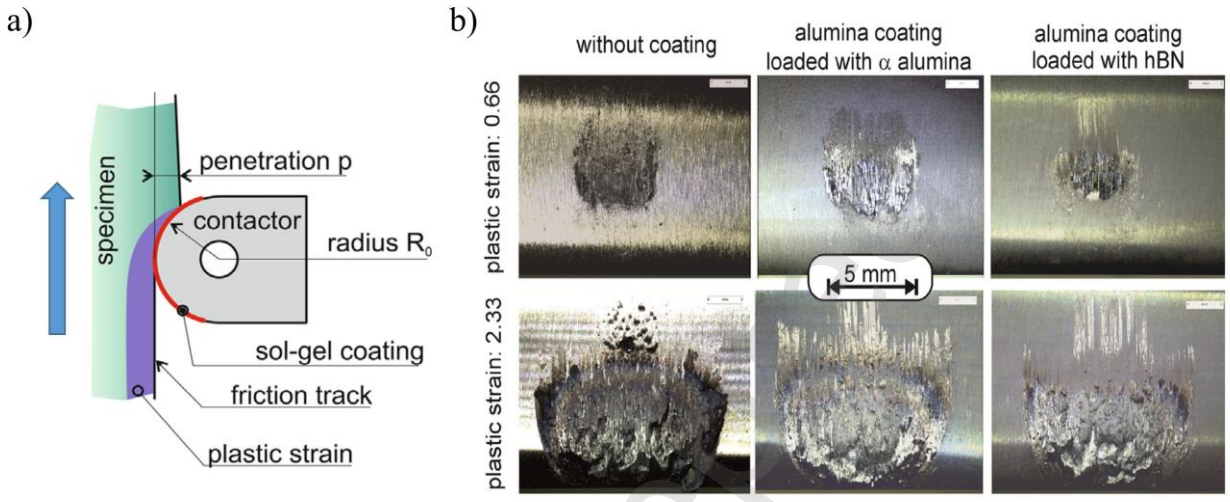

Fig. 24 a) Section view of the contact zone in the warm and hot upsetting sliding test, and b) Friction mark on the contactor surfaces after one test without lubricant [72].

Besides laboratory tribological studies, the performance of nitride coatings was evaluated under real industrial hot forging conditions. For example, Widomski et al. [73] prepared the forging die used in the industrial hot forging process by hybrid surface treatments, which consist of a diffusion nitrided layer combined with thick PVD coatings. The study reported that such hybrid layers increased tool durability by more than 80% compared to conventional treatment. It significantly enhances wear resistance during multi-stage forging operations under complex thermo-mechanical loads. These findings provide important long-term performance validation that complements short-term tribometer data.

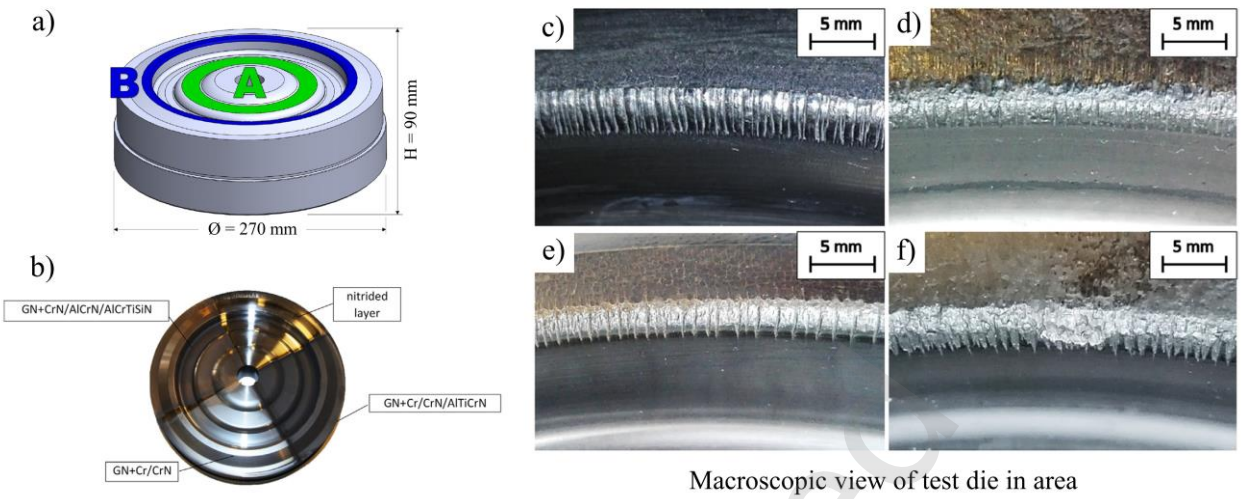

Fig. 25 Application of nitride coating in the hot forging process of steel: a) Die model with the observation zone, b) Forging die with four different surface preparations, and Macroscopic view of die in area "B" after forging of 3,000 cycles: c) GN, d) GN+Cr/CrN, e) GN +Cr/CrN/AlTiCrN, f) GN+CrN/AlCrN/AlCrTiSiN. [74].

Furthermore, Hawryluk et al. [75] reported that the wear resistance of the dies in the hot forging of steel was enhanced by the nitride coating. In their study, a hot forged die was divided into four parts, as shown in Figs. 25a and b. Each part was applied by four different coatings: only nitrided layer (GN), GN+Cr/CrN, GN +Cr/CrN/AlTiCrN, and GN+CrN/AlCrN/AlCrTiSiN. The wear morphology of the coatings was investigated [74,76]. Figures 25c - f compare the state of wear at the 3,000th shot in area "B". It was found that cracks concentrated by abrasive wear on the nitrided layer were observed. In contrast, these cracks on the additional coatings became finer, especially in the layer with Cr/CrN/AlTiCrN coating, where no cracks were observed. It indicates that the multilayered structure coating could reduce the heat transfer between the product and the die, leading to improve the wear resistance of the hot forging die [74].

In addition to mechanical loading conditions, the environment also plays a critical role in the hot forming of steel. These processes are typically conducted in open air at high temperatures, where

rapid oxidation of both the workpiece and the tool surface occurs. The formation and evolution of oxide scales, e.g., FeO, Fe_3O_4, Fe_2O_3, significantly influence interface friction, adhesion, and wear mechanisms. Thus, the tribological performance of coatings under hot forming conditions is closely related to their oxidation resistance and the stability of the oxide layers formed at high temperatures. In this context, environmental effects in hot steel forming are predominantly governed by high-temperature oxidation rather than ambient humidity or others.

For the current application of nitride coatings, the need for coatings is increasing from the viewpoint of tool protection, not only in cold forming but also in hot forming of steels. Coating films and coating technologies are required according to the forming conditions, such as the type of coating, the substrate treatment, and the multilayer structure.

3.2 Hot Forming of Aluminum Alloys

Aluminum products have a wide range of applications, e.g., building materials for housing, due to their formability and corrosion resistance. Extrusion is one of the typical processes used to manufacture aluminum products, such as building materials for housing and frames for aircraft and automobiles. In extrusions of aluminum alloys, the surface quality is required to be more uniform and beautiful than in the past. There is an urgent need for countermeasures against surface defects, such as cracking and warpage. On the other hand, defects, such as pick-up and tearing, have been a major cause of low productivity in actual operations. To increase productivity and improve product quality, it is essential to enhance tribological properties at the die-workpiece interface in addition to conventional extrusion processing technology. This section introduces examples of surface defect generation mechanisms and methods of suppression by the application of nitride coatings.

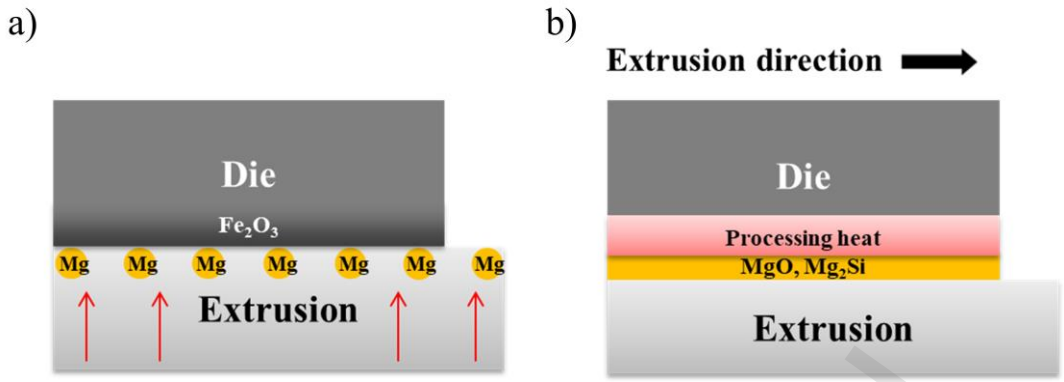

Fig. 26 Schematic diagram of die bearing during hot extrusion: a) Diffusion of Mg and Fe_2O_3, and b) Reaction of Mg and Fe_2O_3 [77,78].

A study on the application of nitride coatings to the bearing surface of hot extrusion dies was conducted to elucidate the mechanism of pick-up defects and their suppression [77]. It was found that the adhesion of an intermetallic compound containing magnesium (Mg) to the die is a major factor in the occurrence of pickup defects. Figure 26 shows the mechanism of adhesion at the die-workpiece interface, resulting in pickup defects [77,78]. As the mechanism of pickup defect generation in the hot extrusion process, work heating occurs due to friction on the bearing surface of the die during extrusion and shear deformation inside the billet. Mg diffuses to the topmost surface at temperatures higher than 300°C [79]. The redox reaction between Mg on the extrudate surface and Fe_2O_3 on the die surface at the bearing area leads to Mg oxides adhering to the bearing surface, and hard intermetallic compounds, such as Mg_2Si, are deposited on the adhered surface with Mg oxides, which are assumed to cause pickup defects due to plucking and separation of the extrudate. To prevent this, it needs to prevent the oxidation of the bearing surface and direct contact between the die and extrudate at the bearing surface. Furthermore, the application of the coating to improve tribological properties on the bearing surface is considered to be effective in suppressing pick-up defects.

As an example of the application of nitride coatings to hot extrusion dies, a friction test simulating the extrusion process is presented by Kalin et al. [80–82]. They conducted a series of studies using a two-cylinder crossed friction tester in which two rods were slid at high temperature. AW6060 aluminum alloy was used as the workpiece, while H13 hot tool steel, without coating, and coated with CrN as well as TiAlN, was used as the die. The friction coefficients were measured at room temperature and at high temperatures between 300°C - 500°C. The TiAlN coating exhibited a particularly low friction coefficient at room temperature. The friction coefficients were similar under hot conditions, whereas the tools coated with TiAlN exhibited less adhesion. This indicates that the TiAlN coating has higher resistance to aluminum in hot forming. Moreover, Birol et al. [83] also performed sliding wear tests on H13 hot tool steel coated CrN, AlTiN, and AlCrN, against AA6063 aluminum alloy. The friction coefficient and the wear in the case of tools coated with AlCrN and TiAlN were lower than those of tools coated with CrN. In particular, the AlTiN coating showed superior performance. This was also confirmed by the findings of Soranansri et al., [84,85]. These studies imply that the application of nitride coatings to the hot forming dies can improve the friction properties and wear resistance. As an approach to nitride coatings for pickup defects, Pellizzari [86] conducted hot sliding tests on AA6082 aluminum alloy to investigate the effect of coatings on pickup occurrence. They showed that the number of pickup defects was greatly reduced in the case of TiAlN and CrN coatings when compared to tool steel without coating and nitriding surface.

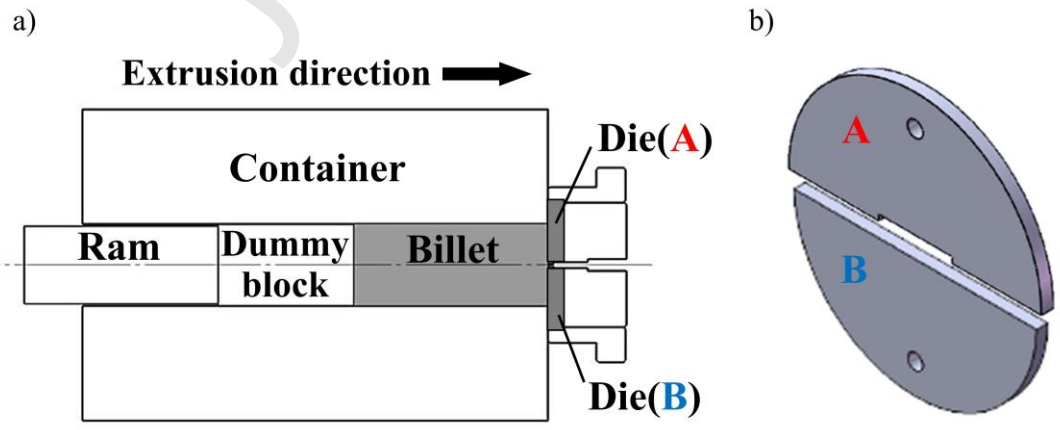

Fig. 27 a) Schematic view of extrusion, and b) Separable die for hot extrusion test [77,78].

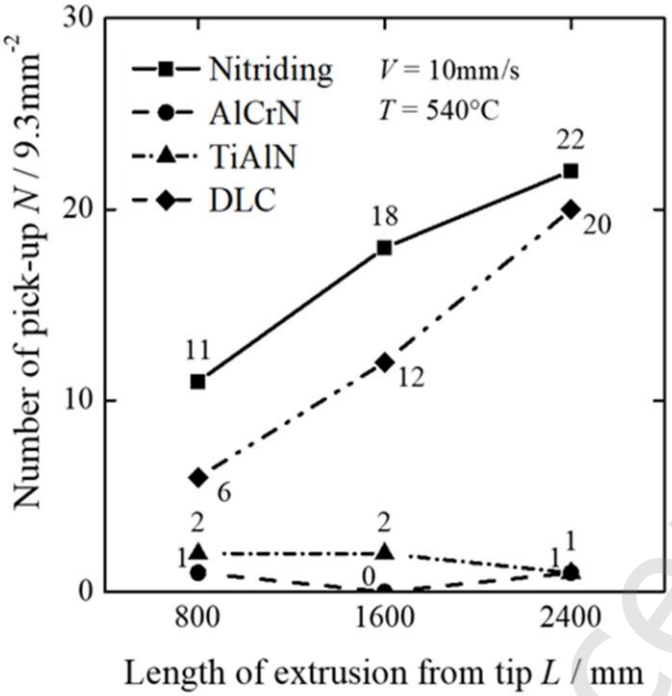

Fig. 28 Number of pick-up in each die coating. (Extrusion temperature 540℃, Ram speed V 10mm/s) [78]

To evaluate the mechanism of pickup defect generation and the effectiveness of coatings, the authors applied nitride coatings to die bearing surfaces as a method to prevent oxidation. When complex-shaped dies with deep holes or constricted areas are targeted, PVD methods, such as ion plating and sputtering, cannot form a uniform coating. Therefore, the molding section was divided, leading to that the coating can be applied evenly to the die bearing section. A split die was used, as shown in Fig. 27. Figure 28 compares the number of pick-up defects up to an extrusion length of 2.4 m from four different coatings on the dies: AlCrN, TiAlN, diamond-like carbon (DLC), and nitriding [78]. The nitriding treatment produced the highest number of pickup defects on the extrudate surface. In the case of DLC, pick-up defects were suppressed in the early stage of extrusion when compared

to the nitriding, but they increased with the progress of extrusion. In contrast, the number of pickup defects in the AlCrN and the TiAlN was very small when compared to the nitriding and the DLC, ranging between 0 - 2 defects at all extrusion distances. The extrudates from the coated dies had a small surface roughness and a shiny surface. Figure 29 shows a monochrome view of the bearing surface appearance of four different coatings [78]. The black areas in the black-and-white figure are the die surfaces, and the white areas are the aluminum alloy. It can be seen that the aluminum alloy on the bearing surface adheres more widely in the order of nitriding > TiAlN > DLC > AlCrN. For both dies, adhesion was observed at the bearing entry area where the surface pressure is high. In the nitriding treatment, a large amount of adhesion due to stop marks was observed at the bearing exit area. It seems that the stop marks were eliminated by applying the coating. The results of the elemental analysis of the bearing surface in these dissimilar coatings show that Mg oxides were formed in the nitriding treatment due to the strong reaction of Mg and the strong reaction of O in the same range; no Mg oxide reaction was observed in AlCrN; no Mg oxide reaction was observed in TiAlN or DLC; and no Mg oxide reaction was observed in AlCrN. Figure 30 presents SEM images of the vacancies caused by droplets on the bearing surface with DLC after aluminum dissolution, their shapes, and the results of Mg, oxygen (O), and carbon (C) surface analysis [78]. The size of the droplet was about 30 μm in diameter and 1.0 μm in depth. Strong reactions of Mg and O were observed in the vacancies, and C, the main component of DLC, was also observed. During extrusion, Mg-containing aluminum alloys are deposited in the vacancies caused by droplets. Since DLC itself is oxidized under high temperature conditions, it is considered that Mg oxides are formed on the oxidized DLC surface with Mg of the aluminum alloy deposited in the vacancies as the extrusion proceeds [87–89]. These results indicate that the deposition of alloying elements, including Mg, on the bearing surface is the cause of pickup defect generation, and that pickup defects could be suppressed by preventing oxidation of the die surface at high temperatures, as in AlCrN and TiAlN.

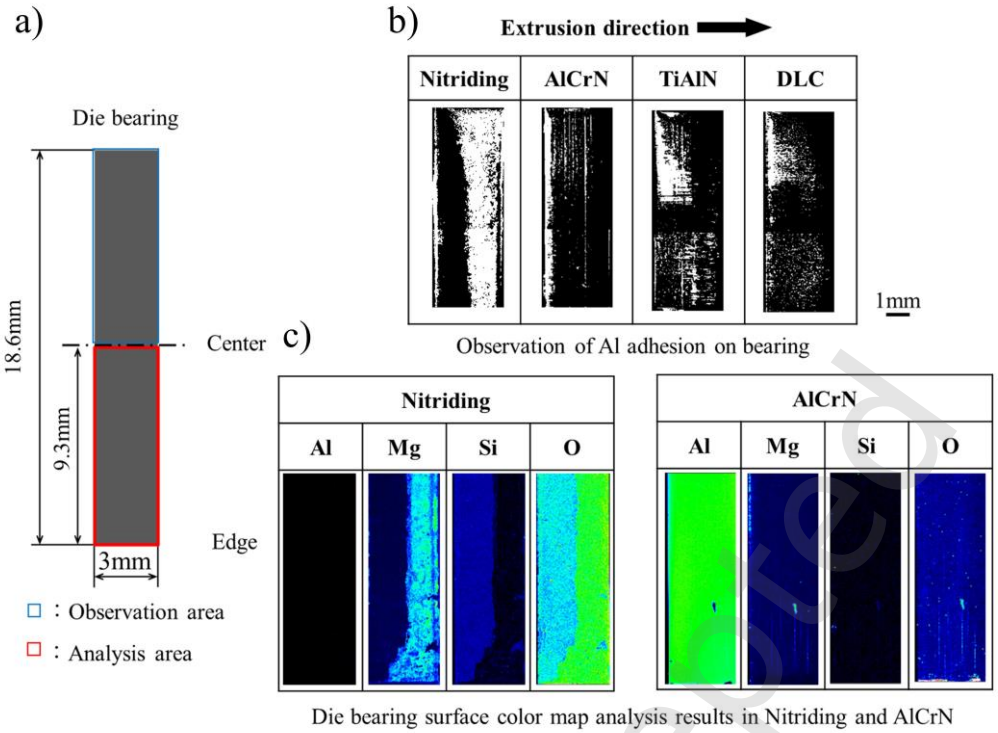

Fig. 29 Die bearing surface after extrusion (Extrusion length 2,400 mm): a) Observation and analysis areas on die bearing surface, b) Observation of aluminum adhesion, and c) Color map of die bearing surface for nitriding and AlCrN [78].

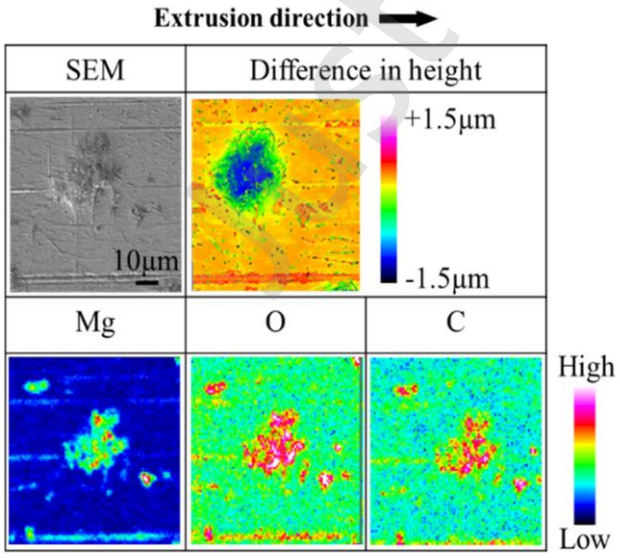

Fig. 30 SEM image, difference in height, and color map analysis results of droplets in DLC. (Extrusion length 2,400 mm) [78]

In addition, Soranansri et al. [90] systematically investigated the mechanisms of aluminum transfer on the DLC-coated forming die using a scale-down of the warm and hot upsetting sliding test [91,92]. This friction test can reproduce the severe thermo-mechanical contact conditions representative of hot bulk aluminum forming. The transfer phenomena can be divided into initial and growth stages, which are summarized schematically in Fig. 31.

During the initial stage, aluminum transfer is caused by mechanical plowing due to the droplets inherent to the DLC coating. These droplets promote localized material accumulation and act as nucleation sites for primary transfer. As sliding proceeds into the growth stage, the transfer mechanism becomes strongly dependent on the contact conditions, particularly interface temperature and relative sliding velocity. In this stage, the dominant mechanism shifts between mechanical plowing and adhesive bonding. Different transfer mechanisms result in dissimilar friction coefficients and surface characteristics of the forming product.

Regarding the effect of the contact condition, increasing the relative sliding velocity reduces adhesive bonding between the primary and secondary transferred layers because the contact time is insufficient to generate strong adhesive junctions, and the higher strain rate also causes the higher yield stress of the aluminum alloy. This leads to the aluminum transfer in the case of higher relative sliding velocity being more predominated by mechanical plowing and a thinner transferred layer on the DLC coating. On the other hand, in the case of lower relative sliding velocity, the interface temperature is the major factor affecting the transfer mechanisms. The higher interface temperature significantly causes more severe adhesive bonding due to the thermal softening of the aluminum alloy and the enhanced chemical affinity between the primary and secondary transferred layers.

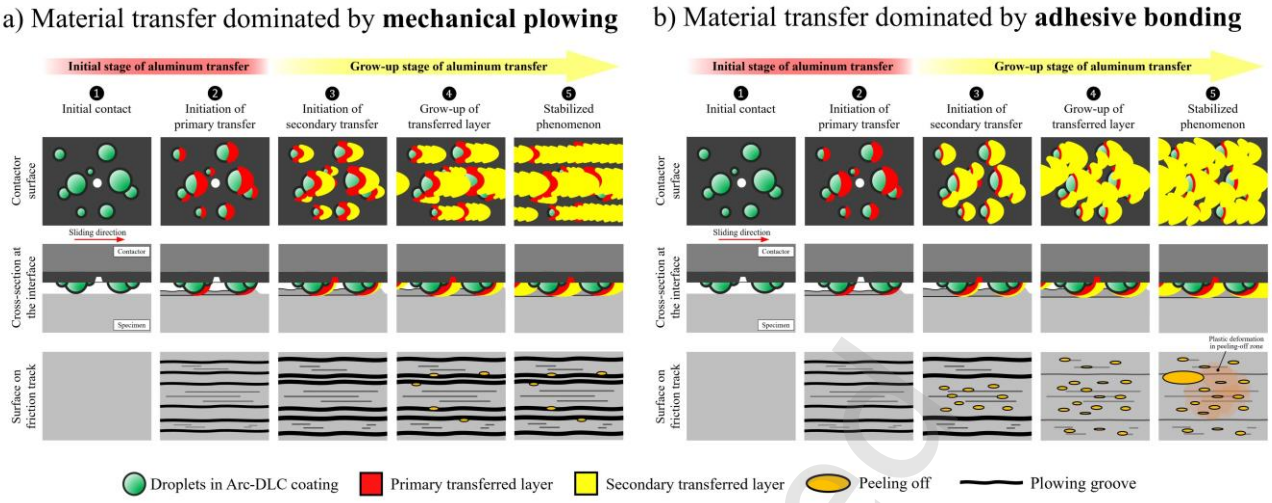

Fig. 31 Mechanism of aluminum transfer on the DLC coating: a) Dominated by mechanical plowing, and b) Dominated by adhesive bonding [90].

7000 series aluminum alloys are high-strength alloys used in various products for weight reduction in the transportation field. In particular, the AA7075 aluminum alloy has the highest strength and is expected to be further applied in a wide range of fields, such as aircraft components and sporting goods. However, the hot extrusion of AAA7075 aluminum alloy significantly limits the extrudate production rate when compared to other aluminum alloys. One of the reasons is the occurrence of a cracking-like defect called tearing on the extrudate surface during the hot extrusion process. Figure 32 shows the tearing mechanism considered by the authors [93]. In the case of AA7075 aluminum alloy, soluble intermetallic compounds, such as Al_2CuMg and $MgZn_2$, locally melt at the grain boundaries and become the starting point of cracking. The cracking is considered to be initiated by local melting of soluble intermetallic compounds, such as Al_2CuMg and $MgZn_2$, at the grain boundaries, and crack propagation is caused by high tensile stress in these areas. Thus, the improvement of tribological properties at the die-workpiece interface by the application of nitride coating is considered as an effective solution in suppressing tearing.

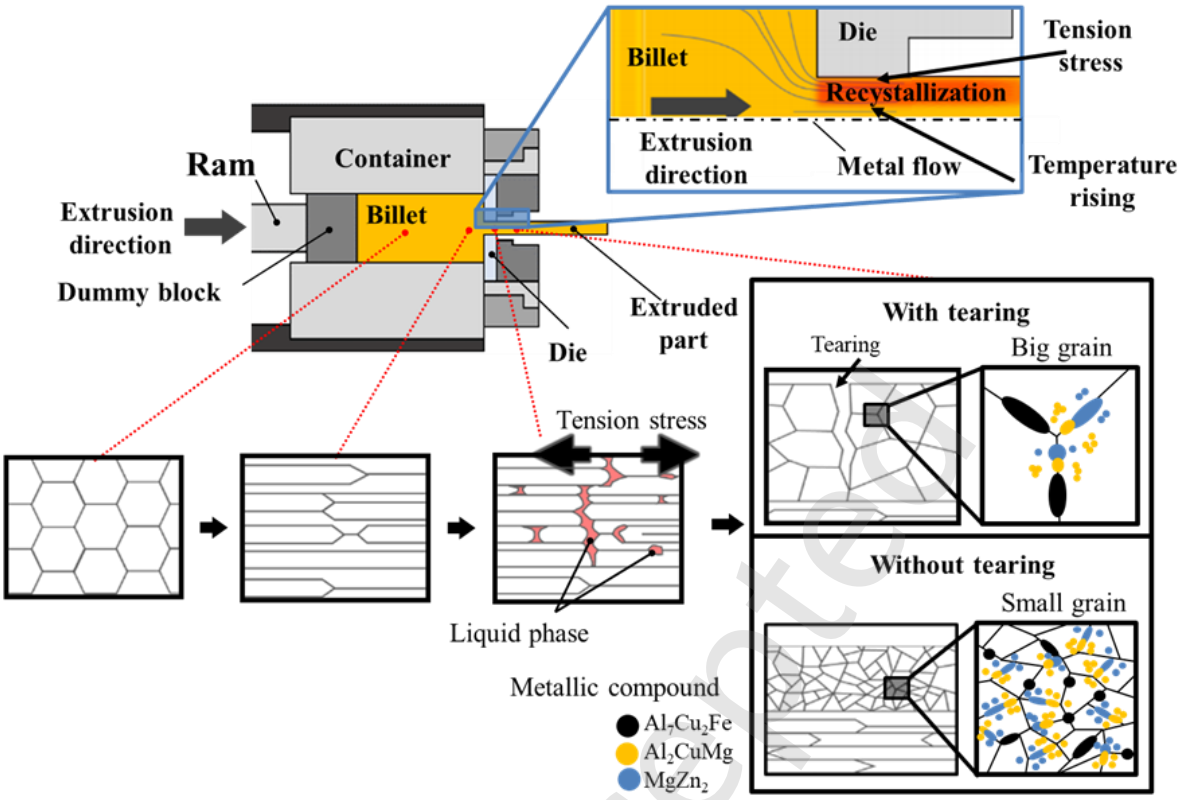

Fig. 32 Tearing defect generation mechanism [93].

The extrudability of alloys used for hot extrusion is evaluated by extrusion limit curves, and the extrusion limit at which tearing occurs is strongly related to the billet temperature and extrusion speed. Figure 33 shows the extrusion limit curve diagrams for tearing defects in AlCrN, TiAlN, DLC, and nitriding [11]. The extrusion limit curves for nitriding and AlCrN are almost the same, while TiAlN and DLC are lower than nitriding and AlCrN. This indicates that these coating films are not effective against tearing. Figure 34 displays the tearing size-stroke diagram for various surface property dies [11]. The tearing is found to increase as the stroke increases. Although the tearing depth increases with stroke for all surface properties, the tearing depth is smaller for AlCrN than for nitrided, TiAlN, and DLC. Figure 35 shows the results of electron beam backscatter diffraction (EBSD) observations of extrudate crystallographic orientation for AlCrN and nitriding [11]. The surface of the profiles was observed at the 3,000 mm point in the second half of the extrudate. Both

extrudate samples were used under the conditions of billet temperature of 450°C and ram speed of 1.0 mm/s. From the EBSD observation results, all extrudate samples showed a grain-like crystal structure at the edge of the extrudate due to recrystallization and a fibrous crystal structure in the center of the extrudate. Comparing the areas where tearing occurred, tearing was observed in the recrystallized layer in both cases, indicating that the cracks occurred along the grain boundaries. The extent of recrystallized layers occurring in the extruded material was smaller with AlCrN than with nitriding, suggesting that AlCrN is a coating with excellent wear and friction resistance and suppressed the increase in tearing depth due to the suppression of processing heat generated during forming.

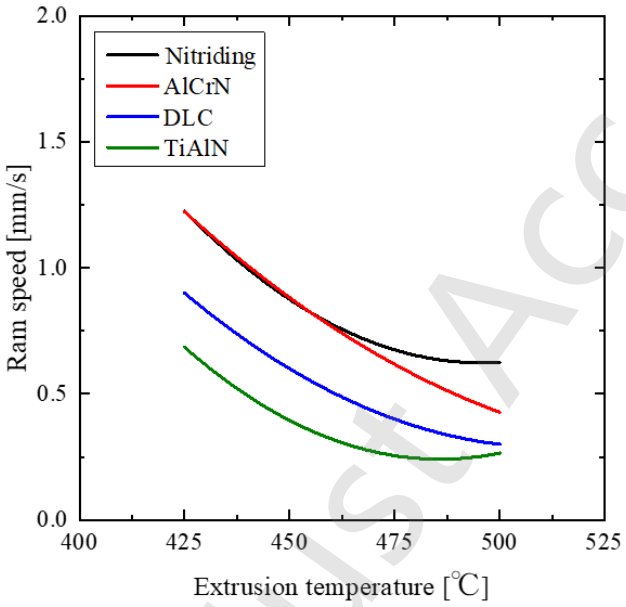

Fig. 33 Extrusion limit curve diagrams for various die coatings of AA7075 aluminum alloy [11].

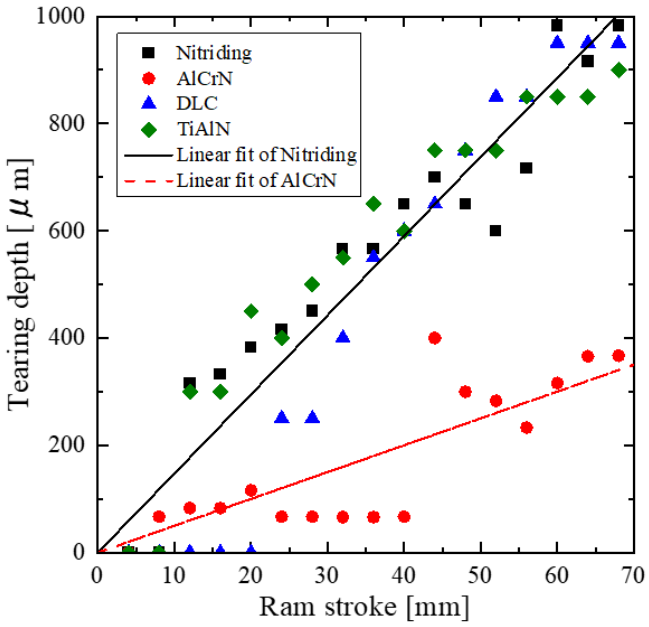

Fig. 34 Tearing defect size and ram stroke in various die coatings (Extrusion speed 1.0 mm/s, Extrusion temperature 450°C, Observation position 2,400 mm) [11].

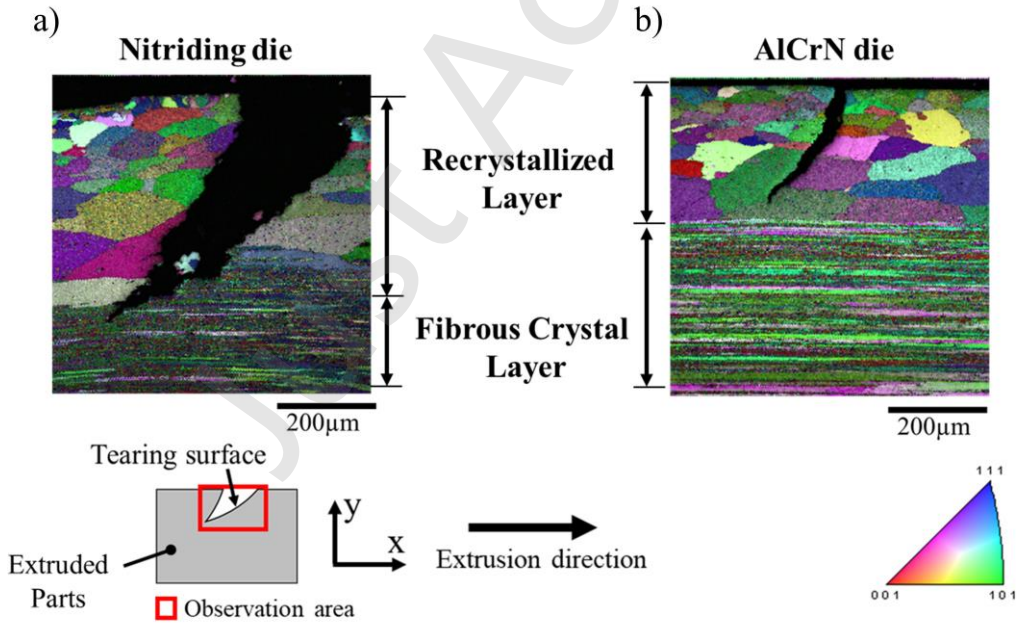

Fig. 35 Extruded surface of AA7075 aluminum alloy: a) Nitriding die and b) AlCrN die (Extrusion speed 1.0 mm/s, Extrusion temperature 450°C, Observation position 2,400 mm) [11].

As a method for identifying the friction coefficient of different coatings in hot extrusion, we proposed a hot forward and backward extrusion friction test method, referring to the report of Hu et al. [94]. From the experimental results at 500°C, nitriding and DLC-coated tools led to a shear friction factor m = 1.0, TiAlN coated tool led to a shear friction factor m = 0.5, and AlCrN coated tool led to a shear friction factor m = 0.2. Figure 36 shows the temperature and principal stress distributions from the hot extrusion analysis with the nitriding and AlCrN die [11]. In the red region of the extrudate temperature, 516°C - 520°C, there is a small amount of AlCrN, but the nitriding treatment is generally large. The temperature distribution at m = 0.2 (AlCrN) is lower than that at m = 1.0 (nitriding). This confirms that a smaller shear friction factor is effective in lowering the working heat generation temperature during hot extrusion and reducing the area of working heat generation in the 516°C - 520°C range.

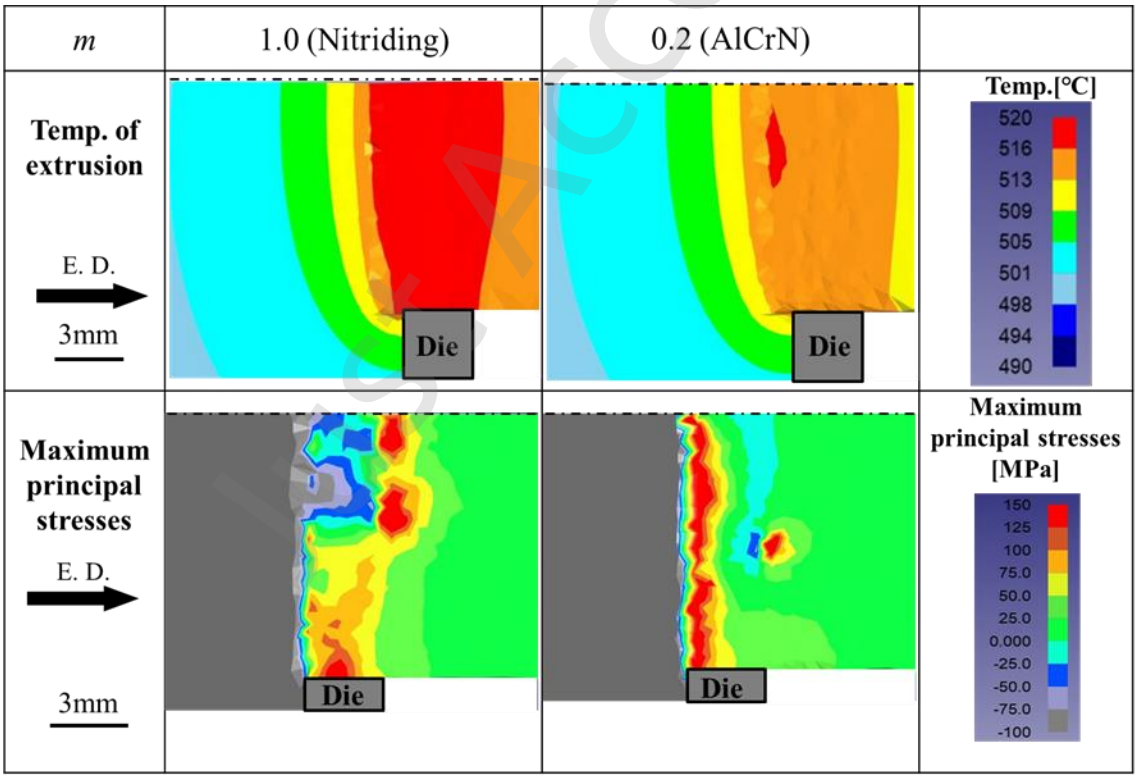

Fig. 36 Temperature distribution and principal stress distribution near bearing in nitrided and AlCrN die [11]

The principal stress distribution from the hot extrusion analysis for nitriding and AlCrN shows that for m = 1.0 (nitriding), the principal stresses near the die bearing area are broadly and non-uniformly distributed. Due to the high degree of deformation at the inner corners of the container, the range of principal stresses at the edge of the extrudate increases as it passes through the corners of the die bearing section. The shear friction factor of m = 1.0 indicates that the billet passes through the die bearing area, and the friction effect on the material flow is significant. The shear friction factor of m = 0.2 (AlCrN) shows that the principal stresses near the die bearing area are uniform only at the die bearing area. Since the shear friction factor is m = 0.2, the effect of friction on the billet as it passes through the die bearing area is reduced, which may improve the material flowability.

The above results indicate that the shear friction factor is significantly related to the occurrence of tearing. The use of AlCrN, which has a shear friction factor m = 0.2, was considered to have the effect of lowering the working heat generation temperature and reducing the area of working heat generation during hot extrusion. In addition, the tearing depth was reduced due to the improvement of material flowability. On the other hand, this did not lead to the suppression of tearing defects themselves. The elimination of tearing defects is strongly influenced by the temperature. Thus, controlling the temperature and crystalline structure of the product is more effective than reducing the heat generation during the forming process.

3.3 Hot Forming of Other Metal Alloys

3.3.1 Magnesium Alloys

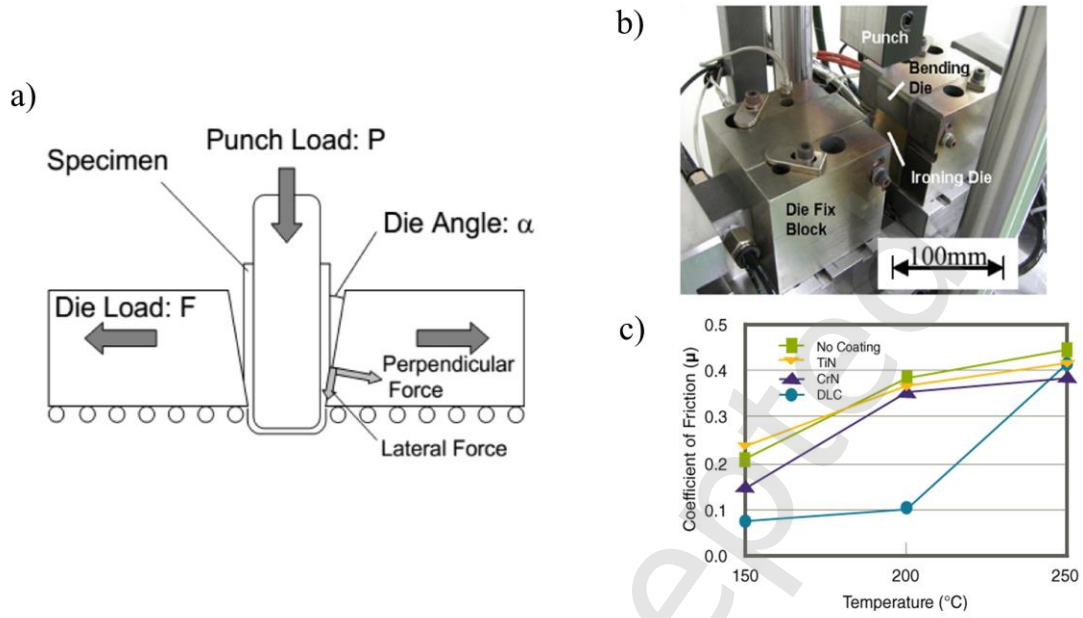

Fig. 37 Friction test of Mg sheet in warm forming: a) Schematic of the U-bending-ironing tribometer, b) Appearance of apparatus, and c) Friction coefficient of different coatings [95].

Magnesium and magnesium alloys, the lightest of all practical metals, are expected to replace aluminum alloys as light metal materials in the near future, especially in the automotive and aircraft industries [96]. Magnesium alloys have limited ductility and high strength at room temperature. Thus, warm or hot forming needs to be applied to shape them [97]. Figure 37 shows the schematic of the U-bending-ironing tribometer, and the results of friction tests on warm plate forming of AZ31 magnesium alloy [95]. In all experimental tests, the DLC coating under no lubricant condition at 150°C - 200°C resulted in a low friction coefficient and a good surface after forming. These results were consistent with a series of studies by Matsumoto et al. [98,99]. Figure 38 presents the schematic of the tapered plug penetration test for AZ31 magnesium alloy and the results. The DLC coating under no lubricant condition at 200°C also provided the low friction coefficient, μ = 0.10, leading to

the lowest maximum penetration load. The adhesion of AZ31 on the DLC coating was less severe than the others [98]. In another study, the results of the ring compression test for ZK60 magnesium alloy indicated that DLC coating at 300°C caused the lowest friction coefficient compared to TiC/TiCN/TiN multi-layer coating and uncoated WC tool [99]. Furthermore, Tsuda et al. [100] evaluated the tribological performance of DLC coating to replace traditional lubricants by using deep-drawing and ironing tests for magnesium alloy sheets. They found that the DLC coating under no lubricant condition at 200°C was comparable to the lubrication condition with MoS_2, etc. From the authors' perspective, magnesium alloy wheels for racing cars and high-end sports cars have been produced by hot forging, and in the future, magnesium alloys will be increasingly used for many applications. Nonetheless, only a few publications focus on tribology using coatings for the hot forming of magnesium alloys.

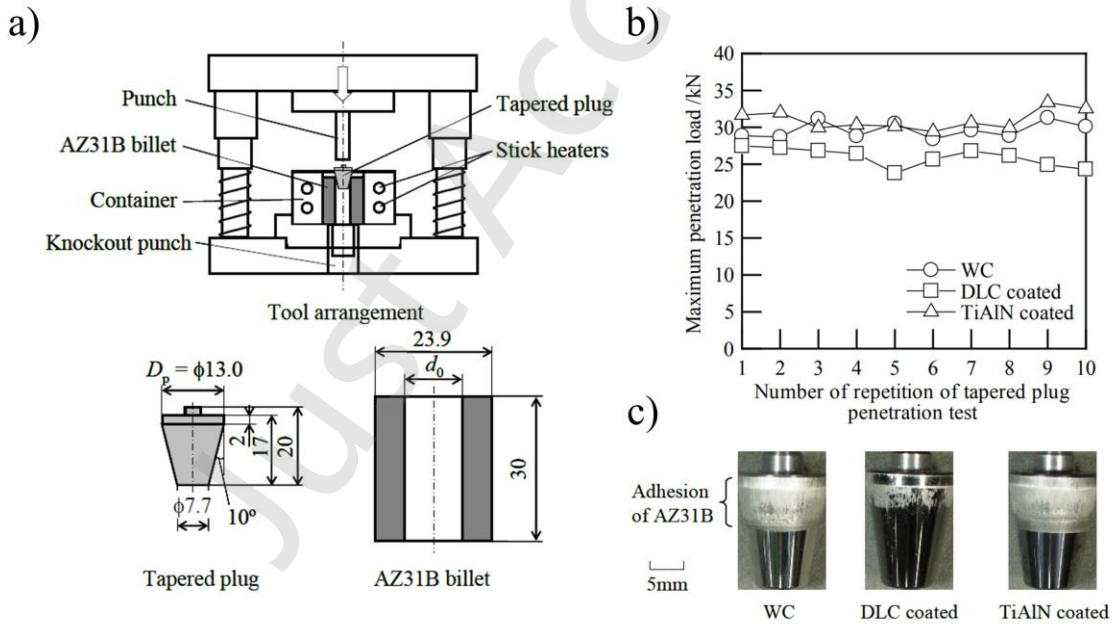

Fig. 38 Friction test of Mg bulk in warm forming: a) Schematic of the tapered plug penetration test, b) Maximum penetration load versus repetition number of the test, and c) Adhesion of AZ31B magnesium alloy on the different coating surface after repetition [98].

3.3.2 Titanium Alloys

A case study of titanium forging by the authors. We developed a thick β-SiC coating for cold forging of pure titanium and austenitic stainless steel [101]. The die with a 4 mm thick β-SiC coating on a SiC substrate was used. Figure 39 presents the SEM and EDX observations of C, Si, O, and Ti on the tool surface after cold forging. It found that the use of a thick β-SiC coating can suppress galling defects due to the self-lubricating effect of C contained in SiC up to a significant reduction in thickness of over 30%, even when forming the pure titanium, which is subject to severe adhesion to the tool. The development of coatings suitable for cold forging should focus not only on the friction coefficient but also on the hardness and thickness of the film itself. From the viewpoint of tool life-lengthening, attention should also be paid to seizure resistance. In another study at room and elevated temperatures, Alpas et al. [88] evaluated the tribological performance of different coatings against Ti–6Al–4V titanium alloy by using a pin-on-disc test. At room temperature, both PCD and H-DLC coatings had friction coefficients of 0.05 and 0.11, respectively (Fig. 40a), which were relatively lower than TiN, TiAlN, and uncoated MS steel. The H-DLC coating could provide low and stable friction from room temperature up to 200°C (Fig. 40b) due to the deterioration of the carbon form at high temperatures [102]. However, the W-DLC coating (W-containing DLC) developed by Alpas et al. could be used at temperatures above 400°C to 500°C (Fig.40c). From the literature review, hardly any publications study the possibility of using coatings for the hot forming of titanium alloys. Moreover, titanium and nickel-based alloys used for aircraft parts are processed at temperatures exceeding 1,000℃. Liquid lubricants cannot be used in such a temperature range, so solid lubricants need to be applied. However, it is difficult for solid lubricants to maintain a uniform lubricant film on the die surface, so coatings that can withstand high temperatures and high contact pressure and the die surface must have high anti-seizing properties.

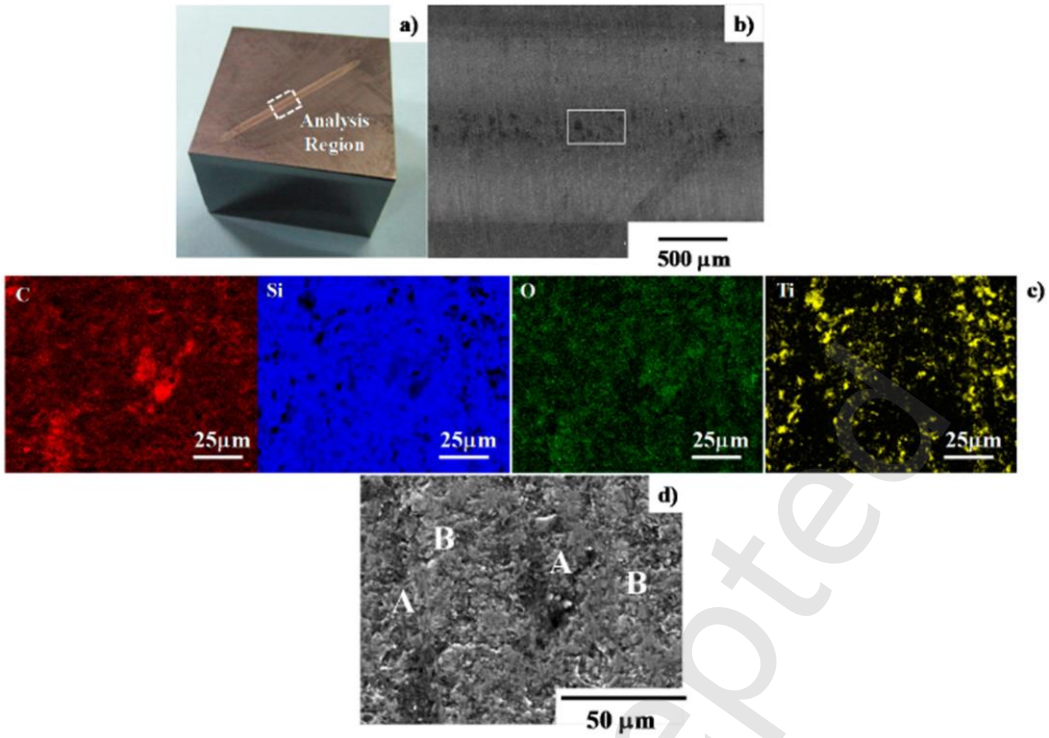

Fig. 39 SEM and EDX analyses at the vicinity of the center of the contact interface between the SiC-coated punch and the titanium wire after forging by 10 shots up to the reduction of the diameter by 35%. a) Optical microscopic image on the SiC coating punch surface; b) SEM image in low magnification on the contact interface of the SiC coating; c) element mapping by C, Si, O, and Ti, and d) SEM image in high magnification at the center of the contact interface (RT., Pure Ti) [101]

.

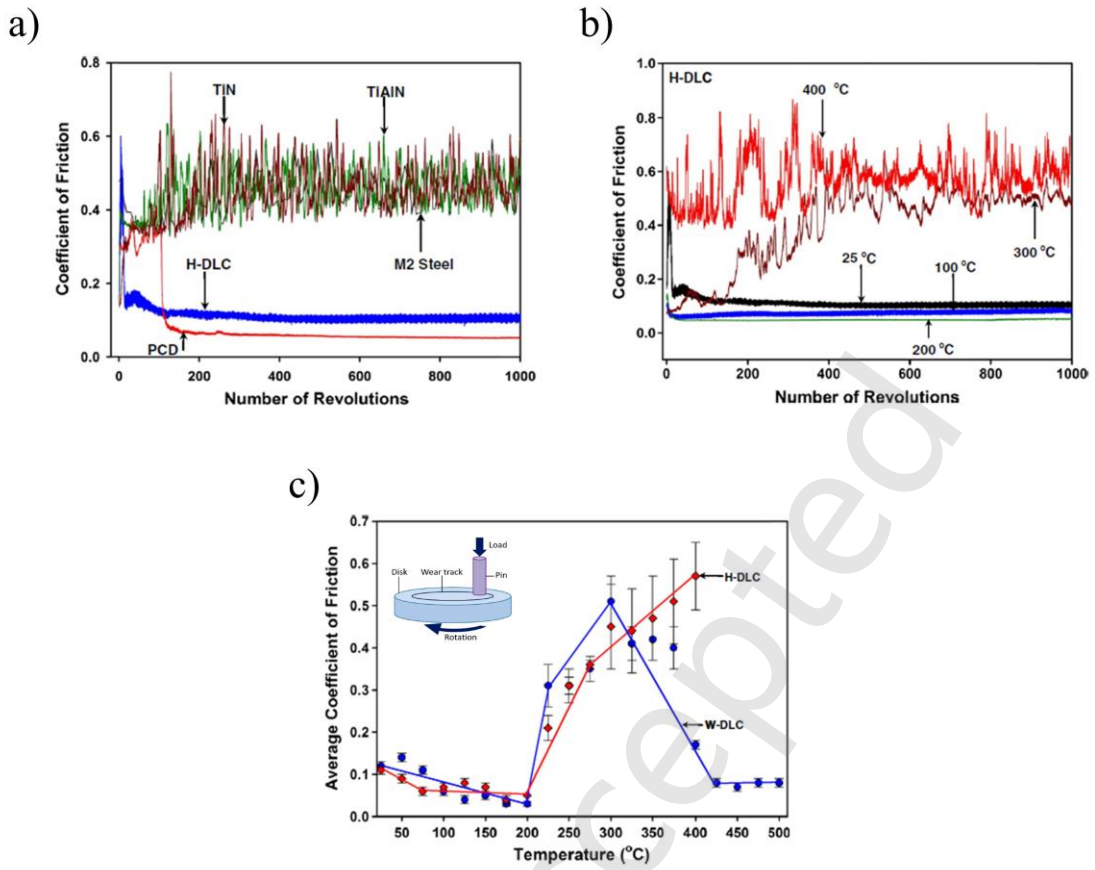

Fig. 40 a) Friction coefficient with the number of revolutions from uncoated M2 steel, TiN, TiAlN, PCD, H-DLC coatings against Ti-6Al-4V at room temperature, b) Friction coefficient with the number of revolutions from H-DLC coating against Ti–6Al–4V from 25°C to 400°C, and c) Average friction coefficient with the testing temperatures for H-DLC and W-DLC coatings [88].

Overall, it was found that the tribological performance of the coating strongly depends on the forming materials: steels, aluminum alloys, magnesium alloys, and titanium alloys. Moreover, friction coefficients and wear characteristics obtained from different tribometers, such as BOD, SRV, WHUST, and strip drawing tests, are not directly comparable due to the dissimilar contact conditions in each tribometer. In hot metal forming, tribological behavior is highly system-dependent and influenced by contact conditions: contact pressure, surface expansion, interface temperature, and sliding velocity. This is because each tribometer is designed to simulate specific contact conditions

of the industrial forming process rather than the complete service condition. Consequently, instead of relying on a single unified friction value, the tribological performance of the coating should be evaluated based on a representative contact condition that reflects the industrial forming application.

All in all, it should be emphasized that most tribological results reported in the open literature are derived from short-duration laboratory experiments, typically one or a few forming cycles. Although those tribometers can simulate the real contact conditions, the dies used in industrial hot forming processes involve repeated thermo-mechanical loading over service life periods. Under such conditions, the coating surface may undergo progressive microstructural evolution, oxidation, wear, and damage accumulation, which cannot be fully captured by short-term laboratory tests [57]. Therefore, the tribological performance observed in laboratory-scale experiments might not completely represent long-term industrial behavior. From this perspective, Future research should focus on long-term and multi-cycle tribological evaluation of nitride coatings under real contact conditions representative of industrial metal forming.

In addition, damaged coatings on forming dies can be repaired in industrial practice. The repairing procedure generally consists of stripping, conditioning, and recoating. At the beginning, the worn or damaged coating layer needs to be removed. To remove the coating layer, there are different stripping methods: chemical technique [103], electrochemical technique [104], and physical technique [105]. These methods can effectively remove the coating and simultaneously prepare a suitable surface for subsequent deposition. After stripping, additional surface conditioning, such as polishing or substrate reconditioning, is required before recoating. Nonetheless, repeated repair cycles may influence substrate, dimensional tolerance, and coating adhesion. Therefore, repairability and lifecycle management should be considered in coating selection for industrial applications of hot forming.

4 Conclusions

In this paper, the design of nitride coatings and their applications for dies and tools used in hot metal forming have been comprehensively reviewed. Therefore, the significant remarks and perspective view for research are concluded as follows:

1) For hot metal forming, both TiN and CrN are commonly used as base systems for nitride coatings. To enhance oxidation resistance and hardness at elevated temperatures, aluminum is often added as a secondary cation to modify from TiN and CrN coatings to TiAlN and CrAlN coatings.

2) The selection of nitride coatings depends mainly on the working temperature and applied load. TiN and TiCN coatings are typically suitable below 423°C under high stress. For intermediate temperatures, 423°C - 723°C, the TiAlN coating is recommended. Nonetheless, CrAlN coating is more reliable at higher temperatures, 673°C - 1,000 °C.

3) Multi-layered and nano-laminated nitride coatings can be an alternative strategy. Their layered structure enhances strength and toughness. This reduces wear by promoting controlled micro-cracking along interfaces, which prevents the coating system from fatal failure. However, the coating structure needs to be designed according to the hot metal forming conditions.

4) For hot forming of steels, the service life of the dies directly depends on the wear resistance at elevated temperatures. Thus, AlCrN and CrWN coatings can be an excellent choice due to their superior wear resistance, which enhances tool durability and performance under high temperatures. On the other hand, for hot forming aluminum alloys, AlCrN and TiAlN coatings are highly effective in reducing surface defects like pick-up and tearing. They can improve frictional properties, resist oxidation, and decrease surface adhesion and frictional heating.

5) For hot forming of magnesium and titanium alloys, DLC coating can provide a low friction coefficient and high surface quality of the workpiece. However, it is important to note that the working temperature is limited due to the deterioration of the carbon form. In the case of titanium

alloys, the forming temperature exceeds 1,000℃. Thus, the nitride coating or other coatings used for the hot forming of both alloys are still in demand.

6) Magnesium alloys are expected to replace aluminum alloys as a light metal in the future, and titanium alloys are also used in numerous applications. Nonetheless, only a few research studies have been conducted on the use of coatings for the hot forming of these alloys, unlike steels and aluminum alloys. Further investigation into the tribological performance of potential coatings used under hot forming conditions is still essential.

7) Future research should focus on long-term and multi-cycle tribological evaluation of coatings under real contact conditions representative of industrial metal forming. Although many specific tribometers developed for metal forming nowadays can simulate contact conditions close to the industrial process, most reported studies remain limited to short-term testing. Systematic investigation of friction evolution, coating degradation mechanisms, and thermal fatigue behavior over extended service cycles is essential to bridge the gap between laboratory assessment and industrial performance.

Acknowledgments

-

Declaration of competing interest

The authors have no competing interests to declare that are relevant to the content of this article.

References

[1] B. Fotovvati, N. Namdari, A. Dehghanghadikolaei, On Coating Techniques for Surface Protection: A Review, Journal of Manufacturing and Materials Processing 3 (2019) 28. https://doi.org/10.3390/jmmp3010028.

[2] M. Piri, H. Hashemolhosseini, R. Mikaeil, M. Ataei, A. Baghbanan, Investigation of wear resistance of drill bits with WC, Diamond-DLC, and TiAlSi coatings with respect to mechanical properties of rock, Int. J. Refract. Metals Hard Mater. 87 (2020). https://doi.org/10.1016/j.ijrmhm.2019.105113.

[3] K. Holmberg, P. Kivikytö-Reponen, P. Härkisaari, K. Valtonen, A. Erdemir, Global energy consumption due to friction and wear in the mining industry, Tribol. Int. 115 (2017) 116–139. https://doi.org/10.1016/j.triboint.2017.05.010.

[4] R. Rajendran, Gas turbine coatings – An overview, Eng. Fail. Anal. 26 (2012) 355–369. https://doi.org/10.1016/j.engfailanal.2012.07.007.

[5] S.L. Semiatin, Metalworking: Bulk Forming, ASM International, 2005. https://doi.org/10.31399/asm.hb.v14a.9781627081856.

[6] I. Serebriakov, E.S. Puchi-Cabrera, L. Dubar, P. Moreau, D. Meresse, J.G. La Barbera-Sosa, Friction analysis during deformation of steels under hot-working conditions, Tribol. Int. 158 (2021). https://doi.org/10.1016/j.triboint.2021.106928.

[7] Z. Gronostajski, M. Kaszuba, S. Polak, M. Zwierzchowski, A. Niechajowicz, M. Hawryluk, The failure mechanisms of hot forging dies, Materials Science and Engineering: A 657 (2016) 147–160. https://doi.org/10.1016/j.msea.2016.01.030.

[8] K. Dohda, C. Boher, F. Rezai-Aria, N. Mahayotsanun, Tribology in metal forming at elevated temperatures, Friction 3 (2015) 1–27. https://doi.org/10.1007/s40544-015-0077-3.

[9] K. Dohda, M. Yamamoto, C. Hu, L. Dubar, K.F. Ehmann, Galling phenomena in metal forming, Friction 9 (2021) 665–685. https://doi.org/10.1007/s40544-020-0430-z.

[10] P. Widomski, M. Kaszuba, D. Dobras, O. Zindulka, Development of a method of increasing the wear resistance of forging dies in the aspect of tool material, thermo-chemical treatment and PVD coatings applied in a selected hot forging process, Wear 477 (2021). https://doi.org/10.1016/j.wear.2021.203828.

[11] T. Funazuka, K. Dohda, N. Takatsuji, C. Hu, N. Sukunthakan, Effect of die coating on surface crack depth of hot extruded 7075 aluminum alloy, Friction 11 (2023) 1212–1224. https://doi.org/10.1007/s40544-022-0649-y.

[12] P. Carlsson, M. Olsson, PVD coatings for sheet metal forming processes—a tribological evaluation, Surf. Coat. Technol. 200 (2006) 4654–4663. https://doi.org/10.1016/j.surfcoat.2004.10.127.

[13] S. Koseki, K. Inoue, S. Morito, T. Ohba, H. Usuki, Comparison of TiN-coated tools using CVD and PVD processes during continuous cutting of Ni-based superalloys, Surf. Coat. Technol. 283 (2015) 353–363. https://doi.org/10.1016/j.surfcoat.2015.10.071.

[14] E. Zdravecká, M. Marton, A. Gmiterko, J. Tkáčová, Tribo-analysis in industry for PVD-coated stamping dies, Tribology in Industry 36 (2014) 3–8.

[15] E. Tomanik, H. Fujita, S. Sato, E. Paes, C. Galvao, P. Morais, Investigation of PVD Piston Ring Coatings With Different Lubricant Formulations, in: Proceedings of the ASME 2017 Internal Combustion Engine Division Fall Technical Conference, American Society of Mechanical Engineers, 2017. https://doi.org/10.1115/ICEF2017-3559.

[16] J.H. Hsieh, A.L.K. Tan, X.T. Zeng, Oxidation and wear behaviors of Ti-based thin films, Surf. Coat. Technol. 201 (2006) 4094–4098. https://doi.org/10.1016/j.surfcoat.2006.08.026.

[17] Akhadejdamrong T., Ph.D. Thesis, University of Tokyo, 2004.

[18] L. Fernandes, F.J.G. Silva, R. Alexandre, Study of TiAlN PVD Coating on Stamping Dies Used in Tinplate Food Package Production, Micromachines (Basel). 10 (2019) 182. https://doi.org/10.3390/mi10030182.

[19] T. Akhadejdamrong, A. Mitsuo, C. Iwamoto, T. Yamamoto, Y. Ikuhara, T. Aizawa, Formation of Protection Layer during Oxidation of Al-Implanted TiN Coating, Mater. Trans. 43 (2002) 1291–1297. https://doi.org/10.2320/matertrans.43.1291.

[20] I. S. Choi, J. C. Park, The corrosion behavior of TiAlN coatings prepared by PVD in a hydrofluoric gas atmosphere, Surf. Coat. Technol. 131 (2000) 383–385. https://doi.org/10.1016/S0257-8972(00)00767-2.

[21] S. Kumar, S.R. Maity, L. Patnaik, Friction and tribological behavior of bare nitrided, TiAlN and AlCrN coated MDC-K hot work tool steel, Ceram. Int. 46 (2020) 17280–17294. https://doi.org/10.1016/j.ceramint.2020.04.015.

[22] W. Tillmann, D. Grisales, D. Stangier, T. Butzke, Tribomechanical Behaviour of TiAlN and CrAlN Coatings Deposited onto AISI H11 with Different Pre-Treatments, Coatings 9 (2019) 519. https://doi.org/10.3390/coatings9080519.

[23] W. Tillmann, M. Dildrop, Influence of Si content on mechanical and tribological properties of TiAlSiN PVD coatings at elevated temperatures, Surf. Coat. Technol. 321 (2017) 448–454. https://doi.org/10.1016/j.surfcoat.2017.05.014.

[24] B. Navinšek, P. Panjan, F. Gorenjak, Improvement of hot forging manufacturing with PVD and DUPLEX coatings, Surf. Coat. Technol. 137 (2001) 255–264. https://doi.org/10.1016/S0257-8972(00)01115-4.

[25] F. Pei, H.J. Liu, L. Chen, Y.X. Xu, Y. Du, Improved properties of TiAlN coating by combined Si-addition and multilayer architecture, J. Alloys Compd. 790 (2019) 909–916. https://doi.org/10.1016/j.jallcom.2019.03.248.

[26] Y. Qiu, S. Zhang, J.-W. Lee, B. Li, Y. Wang, D. Zhao, Self-lubricating CrAlN/VN multilayer coatings at room temperature, Appl. Surf. Sci. 279 (2013) 189–196. https://doi.org/10.1016/j.apsusc.2013.04.068.

[27] E. Aschauer, H. Riedl, C.M. Koller, H. Bolvardi, M. Arndt, P. Polcik, P.H. Mayrhofer, Adhesive wear formation on PVD coated tools applied in hot forming of Al-Si coated steel sheets, Wear 430–431 (2019) 309–316. https://doi.org/10.1016/j.wear.2019.05.019.

[28] H. Ohnuma, N. Nihira, A. Mitsuo, K. Toyoda, K. Kubota, T. Aizawa, Effect of aluminum concentration on friction and wear properties of titanium aluminum nitride films, Surf. Coat. Technol. 177–178 (2004) 623–626. https://doi.org/10.1016/S0257-8972(03)00936-8.

[29] J.A. Thornton, Structure-Zone Models of Thin Films, in: M.R. Jacobson (Ed.), 1988: p. 95. https://doi.org/10.1117/12.941846.

[30] H. Kuwahara, N. Mazaki, M. Takahashi, T. Watanabe, X. Yang, T. Aizawa, Mechanical properties of bulk sintered titanium nitride ceramics, Materials Science and Engineering: A 319–321 (2001) 687–691. https://doi.org/10.1016/S0921-5093(01)00936-4.

[31] A.J. Perry, S.J. Bull, A. Dommann, M. Michler, B.P. Wood, D. Rafaja, J.N. Matossian, The smoothness, hardness and stress in titanium nitride following argon gas cluster ion beam treatment, Surf. Coat. Technol. 140 (2001) 99–108. https://doi.org/10.1016/S0257-8972(01)01008-8.

[32] K. Dohda, T. Aizawa, Tribo-characterization of silicon doped and nano-structured DLC coatings by metal forming simulators, Manuf. Lett. 2 (2014) 82–85. https://doi.org/10.1016/j.mfglet.2014.03.001.

[33] T. Aizawa, H. Kuwahara, M. Tamura, Fabrication of CrN/Cr2N Bulk Composites and Their Mechanical Properties, Journal of the American Ceramic Society 85 (2002) 81–85. https://doi.org/10.1111/j.1151-2916.2002.tb00043.x.

[34] M., Tamura, T., Aizawa, H., Kuwahara, A. Mitsuo, Effect of Chlorine Ion Implantation on CrN Coating in Tribology, in: Heat Treating: Proceedings of the 20th Conference, St. Louis, USA, 2000: pp. 107–114.

[35] L. Rebouta, F. Vaz, M. Andritschky, M.F. da Silva, Oxidation resistance of (Ti, Al, Zr, Si)N coatings in air, Surf. Coat. Technol. 76–77 (1995) 70–74. https://doi.org/10.1016/0257-8972(95)02501-4.

[36] Tsutomu Ikeda, Hiroshi Satoh, Phase formation and characterization of hard coatings in the Ti Al N system prepared by the cathodic arc ion plating method, Thin Solid Films 195 (1991) 99–110. https://doi.org/10.1016/0040-6090(91)90262-V.

[37] H. Windischmann, An intrinsic stress scaling law for polycrystalline thin films prepared by ion beam sputtering, J. Appl. Phys. 62 (1987) 1800–1807. https://doi.org/10.1063/1.339560.

[38] T. Aizawa, J. Kihara, Mechanical characterization of PVD/CVD TiN coated WC/Co by acoustic spectro-microscopy, J. Fac. Eng. Univ. Tokyo (1993).

[39] T. Aizawa, M. Ito, J. Kihara, Quantitative nondestructive evaluation on the ceramic coating by the acoustic spectro microscopy, Japanese J. Tribology. 40 (1995) 171–179.

[40] T Aizawa, 東京大学工学部, 工学系研究科紀要, Acoustic spectro-microscopy for quantitative nondestructive evaluation on the surface structure of materials, J. Fac. Eng. Univ. Tokyo (1997) 127–153.

[41] B.R.E. Pilling N. B., The Oxidation of Metals at High Temperatures, Journal of the Institute of Metals (1923) 529–591.

[42] C. Xu, W. Gao, Pilling-Bedworth ratio for oxidation of alloys, Materials Research Innovations 3 (2000) 231–235. https://doi.org/10.1007/s100190050008.

[43] X. Chen, H. Gao, Y. Bai, H. Yang, Thermal failure mechanism of multilayer brittle TiN/CrAlN films, Ceram. Int. 44 (2018) 8138–8144. https://doi.org/10.1016/j.ceramint.2018.01.260.

[44] H.C. Barshilia, B. Deepthi, N. Selvakumar, A. Jain, K.S. Rajam, Nanolayered multilayer coatings of CrN/CrAlN prepared by reactive DC magnetron sputtering, Appl. Surf. Sci. 253 (2007) 5076–5083. https://doi.org/10.1016/j.apsusc.2006.11.021.

[45] A. Miletić, P. Panjan, M. Čekada, L. Kovačević, P. Terek, J. Kovač, G. Dražič, B. Škorić, Nanolayer CrAlN/TiSiN coating designed for tribological applications, Ceram. Int. 47 (2021) 2022–2033. https://doi.org/10.1016/j.ceramint.2020.09.034.

[46] Y. Chan, H. Chen, J. Duh, J. Lee, Texture, microstructure and tribological behavior in TiAlN/SiNx multilayers, Int. J. Appl. Ceram. Technol. 11 (2014) 611–617. https://doi.org/10.1111/ijac.12060.

[47] M. Stoiber, S. Perlot, C. Mitterer, M. Beschliesser, C. Lugmair, R. Kullmer, PACVD TiN/Ti–B–N multilayers: from micro- to nano-scale, Surf. Coat. Technol. 177–178 (2004) 348–354. https://doi.org/10.1016/j.surfcoat.2003.09.025.

[48] K. Bobzin, High-performance coatings for cutting tools, CIRP J. Manuf. Sci. Technol. 18 (2017) 1–9. https://doi.org/10.1016/j.cirpj.2016.11.004.

[49] G. Abadias, A. Michel, C. Tromas, C. Jaouen, S.N. Dub, Stress, interfacial effects and mechanical properties of nanoscale multilayered coatings, Surf. Coat. Technol. 202 (2007) 844–853. https://doi.org/10.1016/j.surfcoat.2007.05.068.

[50] T. Aizawa, Advanced fracture mechanics design of diamond-like carbon coating against delamination behavior, in: In Recent Trends in Fracture Mechanics, 2012: pp. 323–344.

[51] H.M. Nemat-Nasser S., Micromechanics: overall properties of heterogeneous materials, North-Holland, 1993.

[52] T. Aizawa, E. Iwamura, K. Itoh, Nano-lamination in amorphous carbon for tailored coating in micro-dry stamping of AISI-304 stainless steel sheets, Surf. Coat. Technol. 203 (2008) 794–798. https://doi.org/10.1016/j.surfcoat.2008.08.059.

[53] S.-J. Guo, Q.-S. Yang, X.Q. He, K.M. Liew, Modeling of interface cracking in copper–graphite composites by MD and CFE method, Compos. B Eng. 58 (2014) 586–592. https://doi.org/10.1016/j.compositesb.2013.10.042.

[54] M. Uchida, N. Nihira, A. Mitsuo, K. Toyoda, K. Kubota, T. Aizawa, Friction and wear properties of CrAlN and CrVN films deposited by cathodic arc ion plating method, Surf. Coat. Technol. 177–178 (2004) 627–630. https://doi.org/10.1016/S0257-8972(03)00937-X.

[55] M. Bartosik, R. Hahn, Z.L. Zhang, I. Ivanov, M. Arndt, P. Polcik, P.H. Mayrhofer, Fracture toughness of Ti-Si-N thin films, Int. J. Refract. Metals Hard Mater. 72 (2018) 78–82. https://doi.org/10.1016/j.ijrmhm.2017.12.015.

[56] A. Miletić, P. Panjan, M. Čekada, L. Kovačević, P. Terek, J. Kovač, G. Dražič, B. Škorić, Nanolayer CrAlN/TiSiN coating designed for tribological applications, Ceram. Int. 47 (2021) 2022–2033. https://doi.org/10.1016/j.ceramint.2020.09.034.

[57] N. Bay, A. Azushima, P. Groche, I. Ishibashi, M. Merklein, M. Morishita, T. Nakamura, S. Schmid, M. Yoshida, Environmentally benign tribo-systems for metal forming, CIRP Ann. Manuf. Technol. 59 (2010) 760–780. https://doi.org/10.1016/j.cirp.2010.05.007.

[58] Kenichi Sato, Akihiro Kawano, Shigeru Nakauchi, Hidetaka Goto, Takehiro Kamei, Junichi Tanaka, Development of Light Weight and High-Rigidity Body Structure for All-New Mazda3, 2019.

[59] Y. Yoshida, H. Kanukusa, H. Jinnai, K. Nishihara, H. Fujii, K. Kanayama, K. Okamoto, Research for optimum coating film for press forming of high tensile steel plates and establishment of evaluation method, in: Japanese Joint Conference for the Technology of Plasticity, 2020.

[60] J. Hardell, B. Prakash, High-temperature friction and wear behaviour of different tool steels during sliding against Al-Si-coated high-strength steel, Tribol. Int. 41 (2008) 663–671. https://doi.org/10.1016/j.triboint.2007.07.013.

[61] H. Kim, S. Han, Q. Yan, T. Altan, Evaluation of tool materials, coatings and lubricants in forming galvanized advanced high strength steels (AHSS), CIRP Ann. Manuf. Technol. 57 (2008) 299–304. https://doi.org/10.1016/j.cirp.2008.03.029.

[62] H. Kim, J. Sung, F.E. Goodwin, T. Altan, Investigation of galling in forming galvanized advanced high strength steels (AHSSs) using the twist compression test (TCT), J. Mater. Process. Technol. 205 (2008) 459–468. https://doi.org/10.1016/j.jmatprotec.2007.11.281.

[63] E. Aschauer, H. Riedl, C.M. Koller, H. Bolvardi, M. Arndt, P. Polcik, P.H. Mayrhofer, Adhesive wear formation on PVD coated tools applied in hot forming of Al-Si coated steel sheets, Wear 430–431 (2019) 309–316. https://doi.org/10.1016/j.wear.2019.05.019.

[64] S. Mozgovoy, L. Alik, J. Hardell, B. Prakash, Material transfer during high temperature sliding of Al-Si coated 22MnB5 steel against PVD coatings with and without aluminium, Wear 426–427 (2019) 401–411. https://doi.org/10.1016/j.wear.2018.12.042.

[65] P. Koowattanasuchat, N. Mahayotsanun, S. Mahabunphachai, K. Dohda, Influences of contact pressure, sliding velocity, lubricant, bending angle and surface texture on friction behaviours in stainless steel strip drawing, Advances in Materials and Processing Technologies 1 (2015) 350–360. https://doi.org/10.1080/2374068X.2015.1133744.

[66] S. Mozgovoy, J. Hardell, B. Prakash, High temperature friction and wear studies on tool coatings under press hardening contact conditions, in: 2015.

[67] L. Pelcastre, J. Hardell, B. Prakash, Tribological behaviour of Zn coated UHSS sliding against hot-work tool steel at high temperatures, Wear 376–377 (2017) 423–432. https://doi.org/10.1016/j.wear.2016.10.029.

[68] S. Mozgovoy, L. Alik, J. Hardell, B. Prakash, Material transfer during high temperature sliding of Al-Si coated 22MnB5 steel against PVD coatings with and without aluminium, Wear 426–427 (2019) 401–411. https://doi.org/10.1016/j.wear.2018.12.042.

[69] B. Sresomroeng, V. Premanond, P. Kaewtatip, A. Khantachawana, A. Kurosawa, N. Koga, Performance of CrN radical nitrided tools on deep drawing of advanced high strength steel, Surf. Coat. Technol. 205 (2011) 4198–4204. https://doi.org/10.1016/j.surfcoat.2011.03.010.

[70] E. Vidal-Sallé, M. Dubar, J.C. Boyer, L. Dubar, FEM numerical simulation of the warm and hot upsetting sliding test, International Journal of Material Forming 3 (2010) 315–318. https://doi.org/10.1007/s12289-010-0770-8.

[71] A. Dubois, M. Dubar, L. Dubar, Warm and hot upsetting sliding test: Tribology of metal processes at high temperature, Procedia Eng. 81 (2014) 1964–1969. https://doi.org/10.1016/j.proeng.2014.10.265.

[72] A. Dubois, M. Dubar, C. Debras, K. Hermange, C. Nivot, C. Courtois, New environmentally friendly coatings for hot forging tools, Surf. Coat. Technol. 344 (2018) 342–352. https://doi.org/10.1016/j.surfcoat.2018.03.055.

[73] P. Widomski, M. Kaszuba, D. Dobras, O. Zindulka, Development of a method of increasing the wear resistance of forging dies in the aspect of tool material, thermo-chemical treatment and PVD coatings applied in a selected hot forging process, Wear 477 (2021). https://doi.org/10.1016/j.wear.2021.203828.

[74] Z. Gronostajski, M. Kaszuba, P. Widomski, J. Smolik, J. Ziemba, M. Hawryluk, Analysis of wear mechanisms of hot forging tools protected with hybrid layers performed by nitriding and PVD coatings deposition, Wear 420–421 (2019) 269–280. https://doi.org/10.1016/j.wear.2019.01.003.

[75] M. Hawryluk, Review of selected methods of increasing the life of forging tools in hot die forging processes, Archives of Civil and Mechanical Engineering 16 (2016) 845–866. https://doi.org/10.1016/j.acme.2016.06.001.

[76] M. Hawryluk, Z. Gronostajski, P. Widomski, M. Kaszuba, J. Ziemba, J. Smolik, Influence of the application of a PN+Cr/CrN hybrid layer on the improvement of the lifetime of hot forging tools, J. Mater. Process. Technol. 258 (2018) 226–238. https://doi.org/10.1016/j.jmatprotec.2018.03.029.

[77] T. Funazuka, N. Takatsuji, T. Tsuchiya, S. Oda, Pick-up defect mechanism in hot extrusion of Al-Mg-Si series alloy, Journal of Japan Institute of Light Metals 70 (2020) 415–421. https://doi.org/10.2464/jilm.70.415.

[78] T. Funazuka, N. Takatsuji, K. Dohda, Y. Watanabe, Suppression of pick-up defects in hot extrusion of 6063 aluminum alloy by using PVD coating die, Journal of Japan Institute of Light Metals 70 (2020) 510–516. https://doi.org/10.2464/jilm.70.510.

[79] V.B. Trindade, U. Krupp, Ph.E. -G. Wagenhuber, H. -J. Christ, Oxidation mechanisms of Cr-containing steels and Ni-base alloys at high-temperatures –. Part I: The different role of alloy grain boundaries, Materials and Corrosion 56 (2005) 785–790. https://doi.org/10.1002/maco.200503879.

[80] J. Jerina, M. Kalin, Initiation and evolution of the aluminium-alloy transfer on hot-work tool steel at temperatures from 20 °C to 500 °C, Wear 319 (2014) 234–244. https://doi.org/10.1016/j.wear.2014.07.021.

[81] J. Jerina, M. Kalin, Aluminium-alloy transfer to a CrN coating and a hot-work tool steel at room and elevated temperatures, Wear 340–341 (2015) 82–89. https://doi.org/10.1016/j.wear.2015.07.005.

[82] M. Kalin, J. Jerina, The effect of temperature and sliding distance on coated (CrN, TiAlN) and uncoated nitrided hot-work tool steels against an aluminium alloy, Wear 330–331 (2015) 371–379. https://doi.org/10.1016/j.wear.2015.01.007.

[83] Y. Birol, Sliding wear of CrN, AlCrN and AlTiN coated AISI H13 hot work tool steels in aluminium extrusion, Tribol. Int. 57 (2013) 101–106. https://doi.org/10.1016/j.triboint.2012.07.023.

[84] P. Soranansri, A. Dubois, P. Moreau, T. Funazuka, K. Dohda, L. Dubar, Tribological performance of AlCrN and TiAlN coatings in aluminum forming process at high

temperature, in: Solid State Phenomena, Trans Tech Publications Ltd, 2025: pp. 89–97. https://doi.org/10.4028/p-fICWv5.

[85] P. Soranansri, A. Dubois, P. Moreau, T. Funazuka, K. Dohda, L. Dubar, Tribological Performance of AlCrN, TiAlN, and Arc-DLC Coatings in Hot Forming of Aluminum Alloy †, Lubricants 13 (2025). https://doi.org/10.3390/lubricants13100430.

[86] M. Pellizzari, High temperature wear and friction behaviour of nitrided, PVD-duplex and CVD coated tool steel against 6082 Al alloy, Wear 271 (2011) 2089–2099. https://doi.org/10.1016/j.wear.2011.01.067.

[87] A.A. Gharam, M.J. Lukitsch, M.P. Balogh, N. Irish, A.T. Alpas, High temperature tribological behavior of W-DLC against aluminum, Surf. Coat. Technol. 206 (2011) 1905–1912. https://doi.org/10.1016/j.surfcoat.2011.08.002.

[88] A. Banerji, S. Bhowmick, A.T. Alpas, High temperature tribological behavior of W containing diamond-like carbon (DLC) coating against titanium alloys, Surf. Coat. Technol. 241 (2014) 93–104. https://doi.org/10.1016/j.surfcoat.2013.10.075.

[89] D.-Y. Wang, C.-L. Chang, W.-Y. Ho, Oxidation behavior of diamond-like carbon films, 1999. www.elsevier.nl/locate/surfcoat.

[90] P. Soranansri, A. Dubois, P. Moreau, T. Funazuka, K. Dohda, L. Dubar, Initial and grow-up stages of material transfer on Arc-DLC coating in aluminum forming processes at high temperatures, Wear 556–557 (2024). https://doi.org/10.1016/j.wear.2024.205491.

[91] P. Soranansri, A. Dubois, P. Moreau, T. Funazuka, K. Dohda, L. Dubar, Identification of coulomb and constant shear frictions in hot aluminum forming by using warm and hot upsetting sliding test, International Journal of Material Forming 17 (2024) 55. https://doi.org/10.1007/s12289-024-01858-4.

[92] P. Soranansri, A. Dubois, P. Moreau, L. Dubar, Consideration of pile-up material on identification of friction coefficient in aluminum forming processes at high temperature,

Proceedings of ICTP 2023 - Current Trends in the Technology of Plasticity (2024) 292–300. https://doi.org/10.1007/978-3-031-41341-4_30.

[93] S. Ngernbamrung, T. Funazuka, N. Takatsuji, S. Murakami, K. Dohda, Tearing mechanism for high-strength Al–Zn–Mg–Cu alloys in hot extrusion, Journal of Japan Institute of Light Metals 68 (2018) 660–666. https://doi.org/10.2464/jilm.68.660.

[94] C. Hu, Q. Yin, Z. Zhao, A novel method for determining friction in cold forging of complex parts using a steady combined forward and backward extrusion test, J. Mater. Process. Technol. 249 (2017) 57–66. https://doi.org/10.1016/j.jmatprotec.2017.06.001.

[95] K. Dohda, T. Makino, H. Katoh, Tribo-characteristic of coated die against magnesium in ironing process, International Journal of Material Forming 2 (2009) 243–246. https://doi.org/10.1007/s12289-009-0509-6.

[96] M.K. Kulekci, Magnesium and its alloys applications in automotive industry, International Journal of Advanced Manufacturing Technology 39 (2008) 851–865. https://doi.org/10.1007/s00170-007-1279-2.

[97] K. Iwanaga, H. Tashiro, H. Okamoto, K. Shimizu, Improvement of formability from room temperature to warm temperature in AZ-31 magnesium alloy, J. Mater. Process. Technol. 155–156 (2004) 1313–1316. https://doi.org/10.1016/j.jmatprotec.2004.04.181.

[98] R. MATSUMOTO, H. KAWASHIMA, K. OSAKADA, Friction and Adhesion in Dry Warm Forging of Magnesium Alloy with Coated Tools, Journal of Solid Mechanics and Materials Engineering 1 (2007) 397–405. https://doi.org/10.1299/jmmp.1.397.

[99] R. Matsumoto', K. Osakada', Lubrication and Friction of Magnesium Alloys in Warm Forging, n.d.

[100] S. Tsuda, S. Yoshihara, Y. Tsuji, Y. Iriyama, Dry circular cup deep-drawing of AZ31 magnesium alloy sheet with DLC coating, Journal of Japan Institute of Light Metals 60 (2010) 438–443. https://doi.org/10.2464/jilm.60.438.

[101] T. Aizawa, T. Yoshino, K.I. Ito, T. Fukuda, Thick β-SiC CVD-coated SiC die system for dry cold forging of metals, Crystals (Basel). 10 (2020) 1–13. https://doi.org/10.3390/cryst10060539.

[102] W. Ni, Y.-T. Cheng, A.M. Weiner, T.A. Perry, Tribological behavior of diamond-like-carbon (DLC) coatings against aluminum alloys at elevated temperatures, Surf. Coat. Technol. 201 (2006) 3229–3234. https://doi.org/10.1016/j.surfcoat.2006.06.045/Techni.

[103] A. Kretschmer, V. Jaszfi, V. Dalbauer, V. Schott, S. Benedikt, A.O. Eriksson, A. Limbeck, P.H. Mayrhofer, Designing selective stripping processes for Al-Cr-N hard coatings on WC-Co cemented carbides, Surf. Coat. Technol. 472 (2023). https://doi.org/10.1016/j.surfcoat.2023.129914.

[104] S. Marimuthu, A.M. Kamara, D. Whitehead, P. Mativenga, L. Li, Laser removal of TiN coatings from WC micro-tools and in-process monitoring, Opt. Laser Technol. 42 (2010) 1233–1239. https://doi.org/10.1016/j.optlastec.2010.03.016.

[105] L.C. Ardila, C.M. Moreno, J.M. Sánchez, Electrolytic removal of chromium rich PVD coatings from hardmetals substrates, Int. J. Refract. Metals Hard Mater. 28 (2010) 155–162. https://doi.org/10.1016/j.ijrmhm.2009.07.008.

Author biography

Kuniaki DOHDA. He received a Doctor of Engineering from Nagoya University, Japan. He is a professor at the Department of Mechanical Engineering, Northwestern University, USA. His main

research interests are in the interrelated areas of metal forming process tribology, surface engineering, and micro-manufacturing. Currently, he is the president of IRGTM, IFMM, and GRGLMM. He is a fellow of ASME, JSME, and JSTP.

Tatsuhiko AIZAWA. Director, professor at the Surface Engineering Design Laboratory, SIT (Shibaura Institute of Technology), Japan. He received PhD from The University of Tokyo in 1980. He became a research associate, Institute of Aerospace and Aeronautics in 1980, a lecturer in 1985, an associate professor in 1986 and a professor in 1996 till 2004 at the University of Tokyo. After the research professor in the University of Toronto from 2005 to 2008, he has been working as a professor in SIT from 2009 till now. His research interests include the micro-manufacturing, the innovations in manufacturing and materials processing, and, the materials science and engineering. He has published over 800 papers in Japanese and International Journals and over 90 patents. He has received lots of awards from academic societies including the Distinguished Achievement Award, Japan Institute of Metals, 2011, the Gold Medal, 2017, the Achievement Award, 2019, Japan Society of Technology of Plasticity (JSTP), respectively, the best presentation award at the Conference, AWMFT-2021, and the best paper award in 1st place and best presentation award, ICTMP2024. He was elected as an emeritus member on JSTP in 2023.

Tatsuya FUNAZUKA. He is an assistant professor of the Department of Mechanical Engineering, University of Toyama, Japan. His research interests include working towards understanding the hot extrusion and forging of aluminum alloy, tribology in metal forming, and micro-manufacturing.

Panuwat SORANANSRI. He received his Ph.D. in Mechanical Engineering from the LAMIH UMR CNRS 8201, Université Polytechnique Hauts-de-France, Valenciennes, France. He is currently a lecturer and researcher in the Department of Teacher Training in Mechanical Engineering, Faculty of Technical Education, King Mongkut's University of Technology North Bangkok, Bangkok, Thailand. His research focuses on tribology in metal forming processes.

Keishi OKAMOTO.

He received his Ph.D. in Engineering from Hiroshima University. His research expertise is in the development of PVD and CVD coatings for molds and dies, mechanical components, and medical devices. He is currently the general manager of sales for the hard coating division at TOYO Advanced Technologies Co., Ltd.